# PERFORMANCE STUDY OF BIFACIAL MODULE BASED TIME VARYING MULTILEVEL SOLAR PANEL SYSTEM (MSPS)

By

Rokonuzzaman
16121153
Aditya Das
16121147
Md. Mahbub Ali
16121134
Md. Dilshad Zahan Shuvo
16321052

A thesis submitted to the

Department of Electrical and Electronic Engineering

In partial fulfillment of the requirements for the degree of
Bachelor of Science in Electrical and Electronic Engineering

Electrical and Electronic Engineering
Brac University
January 2021

## Declaration

It is hereby declared that

1. The thesis submitted is my/our own original work while completing degree at BRAC University.

2. The thesis does not contain material previously published or written by a third party, except where this is appropriately cited through full and accurate referencing.

3. The thesis does not contain material which has been accepted, or submitted, for any other degree or diploma at a university or other institution.

4. We have acknowledged all main sources of help.

**Student's Full Name & Signature:**

| | |
|---|---|
| **Md. Mahbub Ali**<br>16121134 | **Md. Dilshad Zahan Shuvo**<br>16321052 |
| **Aditya Das**<br>16121147 | **Rokonuzzaman**<br>16121153 |

## Approval

The thesis titled "PERFORMANCE STUDY OF BIFACIAL MODULE BASED TIME VARYING MULTILEVEL SOLAR PANEL SYSTEM (MSPS)" submitted by

1. Md. Dilshad Zahan Shuvo(16321052)
2. Md. Mahbub Ali(16121134)
3. Rokonuzzaman(16121153)
4. Aditya Das(16121147)

of Fall, 2020 has been accepted as satisfactory in partial fulfillment of the requirement for the degree of Bachelor of Science in Electrical and Electronic Engineering on 13th January, 2021

**Examining Committee:**

Supervisor:
(Member)

_____

Dr. Md. Mosaddequr Rahman
Professor and Chairperson, Dept. of EEE
Brac University

Program Coordinator:
(Member)

_____

Dr. Abu S.M. Mohsin
Assistant Professor, Dept. of EEE
Brac University

Departmental Head:
(Chair)

_____

Dr. Md. Mosaddequr Rahman
Professor and Chairperson, Dept. of EEE
Brac University

## Acknowledgement

We are grateful to almighty for giving us the opportunity to complete our thesis under the supervision of Dr. Md. Mosaddequr Rahman whom we would like to thank for his assistance and guidance throughout the whole research. We also want to express our gratitude to Mr. Mohaimenul Islam for helping us in difficult situations and polishing our thesis.

## Abstract

Sun based energy exists in two structures that we can use for electrical change. One is immediate sunlight based on thermal, making a superheated liquid which can be utilized to make steam and turn a turbine. There are sure spots on the Earth that can utilize this innovation and asset, however, they need a ton of direct cloud-free daylight for a long time for every day consistently. The alternate way sun-oriented energy can be utilized is the immediate change of sunlight-based energy to power utilizing photovoltaic. Solar energy is the only major power generation process that does not require a turbine. The sun is the biggest combination reactor in our close planetary system. Sun-powered energy has the guarantee and potential to tackle the energy emergency of Bangladesh, the restricted space for setting enough sun oriented photovoltaic (PV) panels to fulfill the need of city inhabitants arises as a requirement in actualizing sun-based energy framework in thickly populated metropolitan regions. The target of this research is to do a performance study of bifacial module based multilevel solar panel-based system concerning solar time. As the bifacial module outfits energy from both sides of the module, this necessitates unique thought to figure the irradiation on both surfaces of the solar panel module. Overall, the study based on the simulation and calculate the irradiance, the modified version of an isotropic diffused model derived by Liu and Jordan has been applied. In succession, different parameters (view factor, albedo) were needed to be introduced in this model. This research presents a developed model of multilevel solar panel system compatible for urban areas which is capable of increasing 29.40% more yearly electrical output than a typical multilevel mono-facial system.



**Keywords:** bifacial, solar, albedo, view factor, multilevel, system

# Contents

**Organization of the thesis**

This research comprises 4 chapters as a compact performance study of multilevel bifacial solar panel system. Firstly, chapter 1 of this work introduces the necessity and current situation of the energy sector. To add with that, chapter 1 also describes the design function of the system and literature review of the previous work. Secondly, chapter 2 titled as the "Theoretical Background" upholds the academic research knowledge. Furthermore, chapter 3 and 4 mostly discusses the design structure and simulation results of the energy producing rate. Conclusion and results show the comparative analysis of a bifacial and mono-facial solar panel system out. Following contents of the table and figure list are included in the "List of Figures", "List of Tables" with the tag name and page number. Conclusion and the scope for future research discusses the final output and further research necessity for the multilevel bifacial solar system. Appendix "A" and "B" have the source code of the control system to operate the system.

# List of Figures

## List of Tables

# Chapter 1

## 1. Introduction

A power source capable enough to supply energy to fulfill all the demands should be our prime concern. As per the statistical analysis from the previous experiment, currently, there is 85.16% of the total population of Bangladesh being facilitated by the service of the national power grid in terms of covering its electrical supply[1]**.** Solar energy is an immense source and the best process to harness this power is a solar panel system. To serve this purpose, several models of solar panel systems have their own scale of demand in the energy sector. Alongside, photovoltaic cells of a solar panel system can be used to reduce the shortage on any national level urgency.

On the other hand, the urban structure has its own difficulties to maintain that system on a wide scale. Typically, any urban areas are a bit densely populated with a maximum possible peak of high raised buildings with lower space to implant a solar panel system vastly. This particular performance study will describe such a developed multilevel solar panel system suitable enough for the urban areas with an increased efficiency rate. Solar calculation and the energy consumption rate are simulated and calculated to prove its efficiency throughout this work.

In the present work, we have tried to summarize the proposal of the bifacial solar model schematically with component details and specifications alongside. The design structure is consisting of 3 servo motor, a virtual bar, and a steel bar that holds the stack of the bifacial solar panel is operated by a microcontroller. The Control system uses the Real time clock (RTC) to collect local time and calculate sunrise and sunset time. According to the signal of the control system, servo motors rotate the panel to a specific degree. The results of this rotating bifacial system show significant changes in output efficiency than a typical solar panel system.

## 1.1 Background

### 1.1.1 Literature review

In 2013, in the arena of solar energy, Rahman *et al.* were the first one to introduce and innovate the idea of a multilevel mono-facial solar panel system. The system quintessentially proposed the concept of mounting three sequential panels, in a rack, at a fixed distance; which in turn greatly minimizes the floor area. Subsequently, the project showed great promise in its calculation, where it was discovered that the proposed system can generate at least 18% more energy, while also using 33% less area than the conventional solar panel systems. The project suggested in its study that the system can prove to be a beneficial fit for large urban cities, keeping in mind the context of third world countries. Where it is of great hardship to produce solar electricity for the mass population and additionally, the scarcity of available roof spaces to install solar panels remains a concern to this day [2].

Furthermore, a detailed performance analysis a multilevel solar system was conducted and the results that came out of it was in truth, quite remarkable. Firstly, the analysis calculated the solar energy collected by the proposed system during different seasons and compared it to that of a fixed panel system of the same size, where promising results were found. Secondly, the three-panel system leaned more towards efficiency, as it can be operated in a space of just two conventional systems, and the nature of tracking and sliding of the panel inherently made it much more efficient than the single level fixed panel system. To add with that, for the sole purpose of solar tracking, an automated microcontroller was developed. By using a set of equations and prompted signals, the microcontroller was able to calculate the sunrise and sunset time on each day, thus enabling it to track the sun by controlling the motors, to rotate the panels at a fixed time intervals and angles. Next up in the development process, a prototype of a multitiered solar panel system in addition to an automated solar tracker was built. In this implemented experimental design, the system was able to show about 23% more efficiency in generating energy. What made the prospect even more compelling was that the proposed system was quite facile to construct and develop, to begin with, while taking much less floor space to do so. The physical structure of the prototype was made by using stainless steel bar supporting the three panels, built-in with servo motors controlled by a microcontroller to rotate the panel in sync, with the positioning of the sun.

In 2017, Rahman *et al.* altered their approach and implemented an RTC (Real Time Clock) based multitiered solar panel system[17]. In this process, the microcontroller uses the data from the real-time digital clock to read the real-time and dates, and while doing so, it accurately determines the sunrise and sunset times for a given day. As a result, the microcontroller was able to control the circuit which runs servo motors to rotate the solar panels in sync with the meticulously calculated time intervals to track the sun. Moreover, in the case of mono-facial based module, another study was done in the year 2019, incorporating the dual and single-axis solar tracking system. However, the percent difference in total incident energy in one whole year between the single and dual-axis tracker systems are found to be about 3.96%, without considering the cloud effect, which in truth is quite insignificant [3] . On that note, the 2017 study consequently ended up with an idea to use specially designed reflectors for the proposed system, which can further enhance the efficiency of a multitiered solar panel system. This recommendation of specially designed reflectors is key here because, throughout this whole paper we would like to introduce and explore the scope, plausibility, and efficiency in the case of the bifacial-based module in a multitiered solar panel system instead of mono-facial modules, as found in the previously mentioned studies.

The key benefit of using bifacial photovoltaic (PV) modules is that it can accept light on both sides of the panel, which can greatly help to increase the energy effectuation of a solar panel system. The initial researches and studies relating to bifacial PV technology date back to 1960. Unfortunately, despite its tremendous efficacy, the technology remained largely ignored for the next 20 years, except for some applications in Russian satellites. Moreover, the technology gained its traction in the 70s, when researchers from Mexico and Spain conferred their findings of bifacial PV cell research in the much esteemed first European Photovoltaic Solar Energy Conference held in Luxembourg. Moving forward to the 80s, various research groups from Spain started to discover the high efficiency and high-power gain nature of bifacial PV cells, which resulted in an innumerable number of scientific articles in this field[4]. At this very moment, Sandia National Laboratories and the National Renewable Energy Laboratory are intricately studying the bifacial PV performance and characterization in a collaborative project funded by the US Department of Energy.

## 1.2 Aims and Objective Scope of the work

The growing urge for electricity and the cost of its consumption requires the full usage of solar energy or any sort of improved energy producing structure that will not become costly and sufficient to fulfill this urgent demand for electricity. Oil, gas, and coal are the primary fuel in Bangladesh to generate electricity while these are limited natural resources available whereas cosmic energy is more economical and harmless to use this resource. Even after having a lower efficiency rate to produce electricity from solar, it has a wide scope of fulfilling the necessity in our country cost-effectively. Conventional photovoltaic solar panels require a good amount of spacing and proper positioning and the output is not a suitable system to implement widely in urban areas. So, this project demonstration and design implementation represent a developed way of using a typical cosmic panel producing more electricity being independent of huge space and fixed position.

## 1.3 Research methodology

The following research is based on the data collected from the simulation of the proposed bifacial multilevel solar panel system. Later the study compares the result collected from the observation of the simulation and monitored the typical mono-facial solar system electrical output to compare with. During the research and study of the performance of bifacial multilevel solar panel system, a solar panel structure consists of a single diode model for a bifacial solar panel is used and the electrical output generation of bifacial solar panel system is compared in terms of monthly and yearly as a cumulative analysis.

# Chapter 2

## 2. Theoretical Background

### 2.1. Basic Solar cell

The most widely recognized sort of photovoltaic we find on the planet today are made of the component silicon. The sunlight-based cell is the essential unit of a photovoltaic module or board. A single solar cell produces about a large portion of a volt of power and up to around eight amps relying upon the kind of cell[16]. That is around 33% of the voltage of a double-A battery. The solar cell comprises a bit of silicon with contacts or anodes that are put across the surface and on the back.

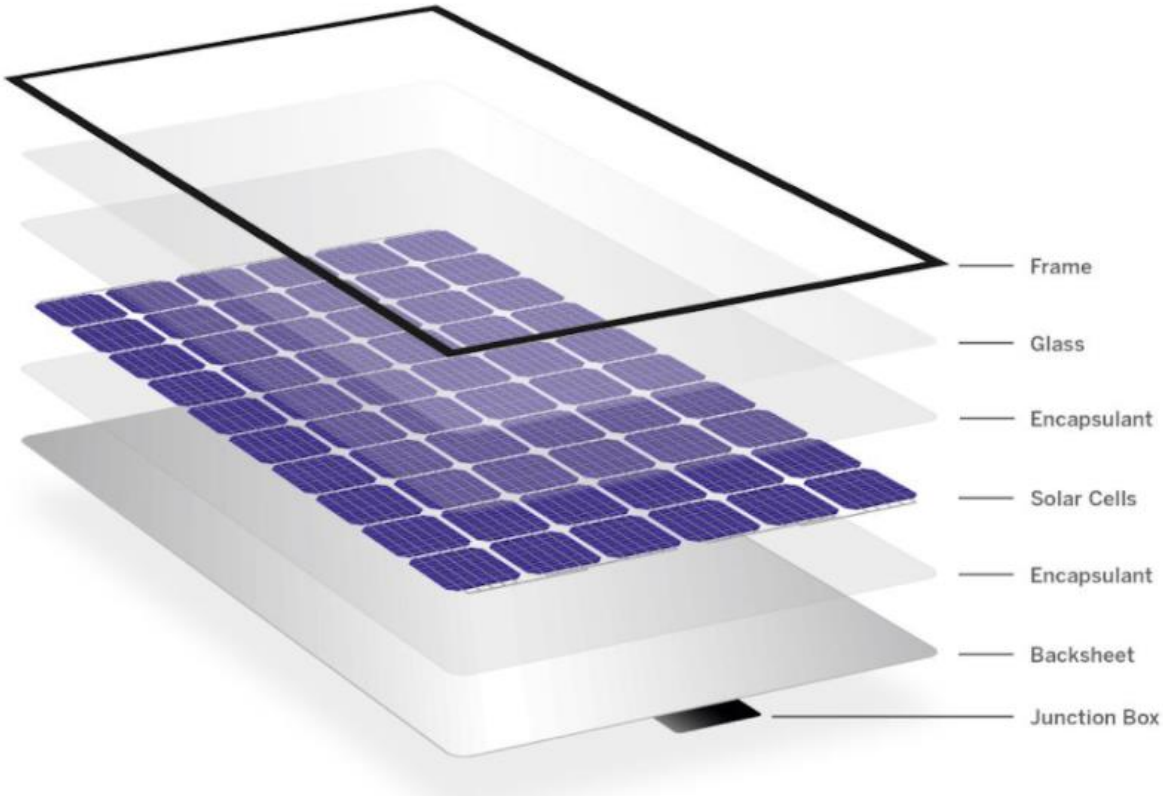


*Figure 1: Solar cell*

Cells are associated in arrangement to make what is known as an arrangement string. Subsequently, expanding the voltage. This is like how batteries are assembled in gadgets, front to back so they amount to a higher voltage. Thus, for instance, we can place two double-A

batteries into an electric lamp, which builds the complete voltage to three volts. The voltage of the arrangement string is basically the amount of the half volt cells, which in this decorated illustration of eight cells would be four volts. The arrangement string is overlaid to the backing material, fixed in a weatherproof plastic covering, and afterwards, a cover glass is set on top, frequently with an aluminum outline around the edges. This assembly is known as the photovoltaic module. It is also referred to as a solar panel.

### 2.1.1. Mono-facial Solar cell

Mono-facial solar panel consists of a single side of solar cells on the surface of the panel considered to be the front surface of the panel. In a mono facial solar panel, the light just enters through one side of the cell. That implies mono facial solar panels can bridle just the direct solar irradiance from the sun. Mono-facial solar panel system is a common model of solar panel system with a lower or adjustable electrical output. Mono-facial solar panels do not harness the reflected irradiance as it is functional to get the direct irradiance and diffusion energy from the sun on a single side.

### 2.1.2. Bifacial Solar cell

In contrast to mono facial solar panels, light can reflect and diffuse from both front and back surfaces of the bifacial sun powered panels. So alongside direct irradiance, diffused and reflected irradiance from the sun can likewise be consumed by a bifacial solar panel. Moreover, the bifacial solar modules offer numerous favorable circumstances over the mono-facial sunlight-based modules. Power can be delivered from the two sides of a bifacial module, expanding the complete energy age. Both side UV resistance makes the modules more lasting.

Equilibrium of framework costs is additionally decreased when more power can be yielded from the bifacial modules in a more modest array impression. Bifacial modules mounted close to a housetop block any reflected light from arriving at the posterior of the cells. That is the reason bifacial modules perform better on level business housetops. It can also be efficient for ground-mounted exhibits on the grounds allowing more space for tilt and reflected light to the backside of the panel.

### 2.1.3. Types of Solar Cell

Solar cells are gadgets that convert light into electricity. They have designated "solar" cells because more often than not, the most impressive wellspring of light accessible is the Sun, called Sol by astronomers. A few researchers call them photovoltaic which implies, fundamentally, "light-electricity." It is a type of photoelectric cell, characterized as a gadget whose electrical attributes—for example current, voltage, or opposition—contrast when exposed to light. At the point when the quantities of the photovoltaic cells are assembled, it will make a solar module that will deliver electric force from sunlight. A solar photovoltaic panel is a mix of various cells in a single panel. The proficiency of most solar panels is from 11-23 percent. The effectiveness rating estimates what level of sunlight striking a panel gets changed over into electricity that can be utilized. The higher productivity, the less surface zone we'll require in our solar panels. Even though the normal rate might be small, we can easily fit an ordinary rooftop with enough capacity to cover our energy needs. There are various kinds of panels and there are varieties in properties among those panels too.

Considering the advantages and disadvantages of the different types of solar panel cells there are 3 different and unique categories are available:

| Solar panel type | Advantages | Disadvantages |
|---|---|---|
| Mono or single crystalline | Highest efficient converting light to electricity, Non-flaky appearance[18] | Expensive |
| Poly or multi-crystalline | Affordable and cheaper, | Less efficient, flaky appearance |
| Thin-film | Portable, lightweight | Low efficiency |

*Table 1:Solar panel Comparison*

## 2.2. Single diode model of bifacial solar cell

The single diode model refers to the model representing the proposed circuit diagram connection to construct a bifacial solar cell. The bifacial solar cell produces more electricity by converting solar energy without any pollution to the environment. To simulate a bifacial solar cell several models as single diode model, two diode model, three diode model, a model with partial shading considerations, and much more were proposed in various works[19]. Among them, a single solar diode model has its own advantage and disadvantage to become a popular model to simulate.

Single diode model in power system planning purpose is more time saving as the parameters are known which decreases the number of iterations to calculate I-V characteristics.

### 2.2.1. Circuit Diagram

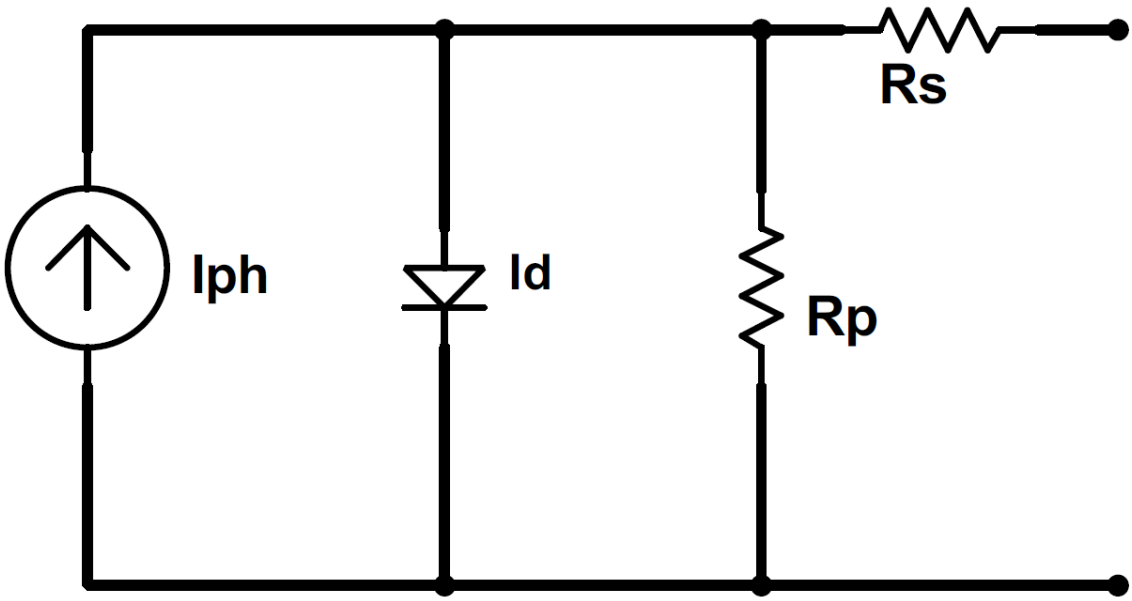


*Figure 2: Single Diode Model*

**Model Description:** Mono-facial cell single diode model of a bifacial solar cell consists of five parameters[6]:

**Shunt resistance ($R_p$ ):** leakage current to the ground caused by the reverse biasing of the diode is characterized by this shunt resistance.

**Series resistance ($R_s$ ):** voltage drops along with internal losses are considered as Rs. In this case, the voltage drops, and the internal losses are caused by the current flow.

**Photocurrent ($I_{ph}$ ):** photon generated the current which can be evaluated for any arbitrary value of irradiance

Reverse saturation current ($I_o$) and diode factor (n) also have an impact to determine PV cell efficiency.

The single cell diode model is represented by the equation

$$I = I_{ph} - I_o\left(e^{\frac{V+IR_S}{n_S V_T}} - 1\right) - \frac{V+IR_S}{R_p}\ [6] \quad \text{----------(1)}$$

Here, $V_T$ Thermal voltage equivalent

However, the single diode model does not consider the recombination effect of a diode which is an obstacle to declare this model as the most accurate model to simulate a solar cell for a complete photovoltaic system .

.

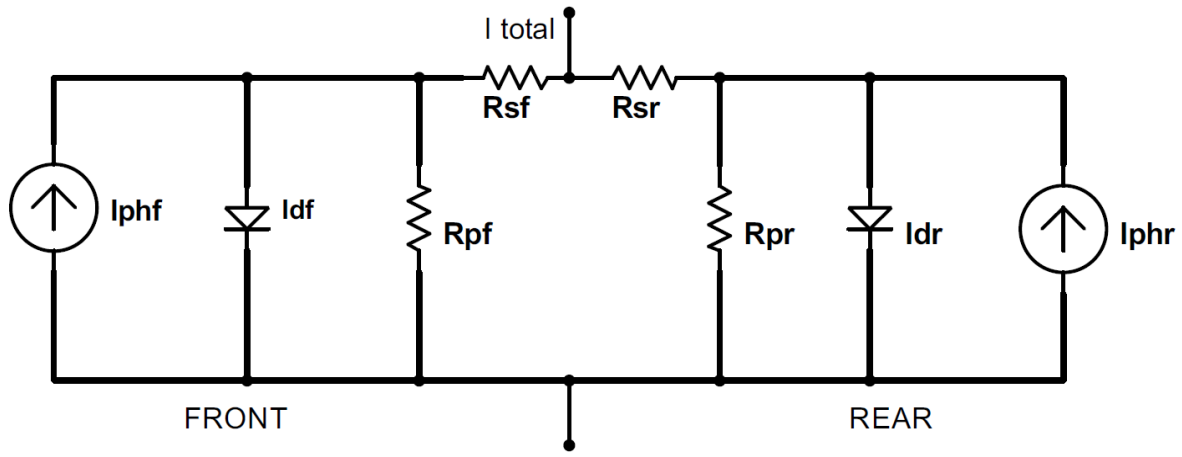


*Figure 3: bifacial technology based Single diode model*

To construct a model for bifacial module, two single diode model for each front and rear is considered to maintain IV characteristics of the module. To illustrate the bifacial technology, two single diode models are placed in parallel. Therefore, for front side total current is calculated by the equation [6][7].

$$I_f = I_{phf} - I_{df} - I_{rpf} \text{ .----------(2)}$$

Where,

$I_{phf}$ = photon generated current,

$I_{df}$ = diode current

$I_{rpf}$ = leakage current

Total generated current for rear side is calculated by the equation

$$I_r = I_{phr} - I_{dr} - I_{rpr} \text{----------(3)}$$

In the figure 2 both front and rear current meet at the same node, so the total current of the single diode model of the bifacial system is $I_{total} = I_f + I_r$ ----------(4)

## 2.3.Solar radiation

### 2.3.1. Extraterrestrial radiation

The starting point for a clear sky radiation calculation is with an estimate of the extraterrestrial (ET) solar insolation , which passes perpendicularly through an imaginary surface just outside of the earth's atmosphere. This insolation depends on the distance between the earth and the sun, which varies with the time of year. In other words, extraterrestrial solar incidence can be described as the amount of solar energy per unit time, at the mean distance of the earth from the sun, received on a unit area of a surface normal to the sun. Sun rays that reach to earth's surface are normally the radiance other than the portion of the total radiation that is lost during the path through the atmosphere [8].

So, total irradiance emitting from the sun or the extraterrestrial irradiance is the summation of the solar radiance blocked by the atmosphere and the available irradiance on the surface [9]

$$G_{on} = G_{sc} * (1 + 0.033cos\frac{360n}{365})\text{----------(5)}$$

In equation no. (5) , $G_{on}$is the extraterrestrial radiation incident on the plane on the nth day of the year. Here the, the solar constant $G_{sc}\ is\ 1367w/m^2$.

### 2.3.2. Definition

Extraterrestrial radiation *:* Solar radiation incident outside the earth's atmosphere is called extraterrestrial radiation.

Solar constant ($G_{sc}$): solar constant is the energy from the sun per unit time received on a unit area of surface perpendicular to the direction of propagation of the radiation at mean earth-sun distance outside the atmosphere.

Beam Radiation*:* The solar radiation received from the sun without having been scattered by the atmosphere [8].

Air mass: (m): The ratio of the mass of atmosphere through which beam radiation passes to the mass it would pass through if the sun were at the zenith.

Diffuse Radiation: The solar radiation received from the sun after its direction has been changed by scattering by the atmosphere.

Irradiance (W/m2) : The rate at which radiant energy is incident on a surface per unit area of surface.

Latitude(L): The angular location north or south of the equator, north positive.

Slope(β): The angle between the plane of the surface in question and the horizontal.

Surface azimuth angle(γ)*:* the deviation of the projection on a horizontal plane of the

normal to the surface from the local meridian, with zero due south, east negative, and

west positive.

Angle of incidence(θ): The angle between the beam radiation on a surface and the normal to that surface.

Zenith angle($\theta_z$): The angle between the vertical and the line to the sun, that is, the angle.

of incidence of beam radiation on a horizontal surface.

Solar altitude angle($\alpha_s$): The angle between the horizontal and the line to the sun that is, the complement of the zenith angle.

Solar azimuth angle($\gamma_s$): the angular displacement from south of the projection of beam.

Declination angle(δ): The angular position of the sun at solar noon. The angular position of the sun at solar noon , $\boldsymbol{\delta}$ can be calculated by the derived equation given below,

$$\delta = 23.45° \sin\left[\frac{n+284}{365} * 360°\right] \text{----------(6)}$$

This particular declination angle is calculated on the nth day of the year.

Hour angle (H): The angular displacement of the sun east or west of the local meridian due to rotation of the earth on its axis at 15◦ per hour; morning negative, afternoon positive [8].

From the perspective of northern hemisphere, hour angle is negative from the sunrise time $S_r$, $H_s$ is the sunrise angle and t are the time of a day in 24-hour format clock.

$$H = -H_s + 2\frac{H_s}{T}(t - S_r)$$ ----------(7)

$$H_s = cos^{-1}(-tan\delta . tan\gamma)$$----------(8)

Altitude:

Altitude angle is the angle between the sun and the local horizon directly beneath the sun. The formula of solar altitude angle($\alpha_S$) combines with latitude($L$), declination angle($\delta$) and hour angle ($H$)[12].The equation is known as,

$$\text{Cos}\,(\theta_z) = Sin(\alpha_S) = Cos(L)Cos(\delta)Cos(H) + Sin(L)Sin(\delta)$$----------(9)

Zenith angle ($\theta_Z$) and the azimuth angle (γ) is necessary to calculate the total angle of incidence

$$\theta_z = 90° - \alpha_S$$ ----------(10)

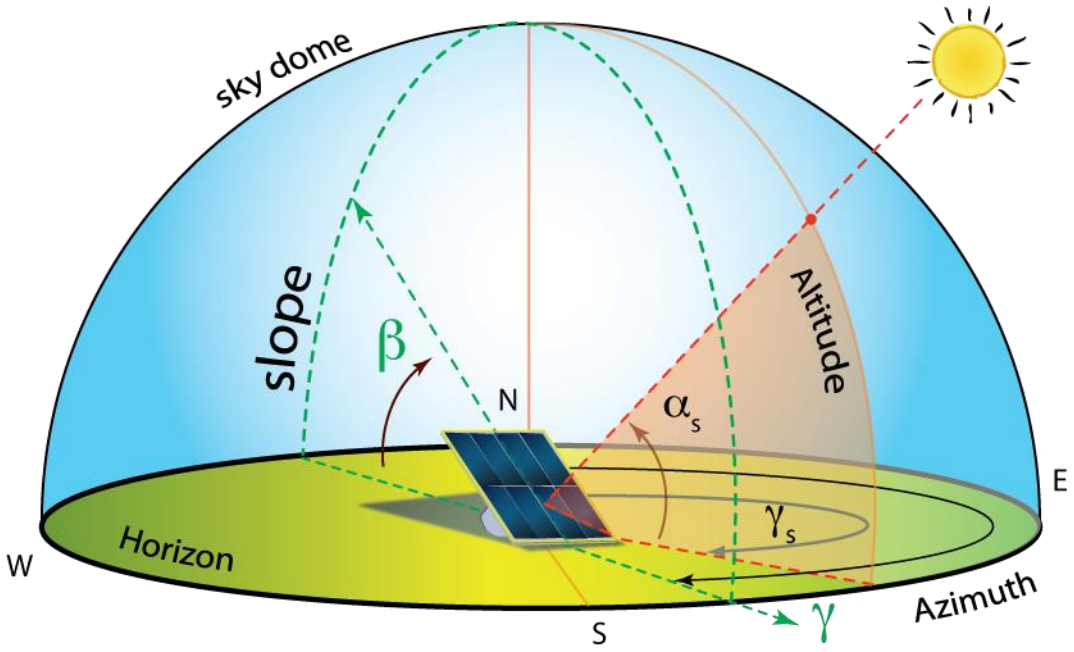


*Figure 4: Solar angle*

radiation on the horizontal plane, shown in Figure 4 Displacements east of south are negative and west of south are positive.

### 2.3.3. Irradiation Model

Initially tried to model a system compatible enough to harness all the radiation on a collector panel. The irradiation from the sun is divided into two section termed as the Direct irradiation and the other one is reflection. Estimating the diffusion energy which is scattered by the atmosphere is quite harder as the weather condition, geographic location has its own impacts on the rate of diffusion. The last component of the isotropic model is the ground reflected irradiation by the surface of the earth and by any other surroundings.
An isotropic model was derived by Liu and Jordan. Later a modified model was developed by THRELKELD and JORDAN which was used in ASHRAE solar day clear flux model[9].

Total components of solar irradiance can be composed as;

- Beam,
- Isotropic diffuse,
- Diffusely reflected from the ground.

#### 2.3.3.1. Liu and Jordan model

The proposed model of Liu & Jordan, published in The Interrelationship and characteristic Distribution of Direct, Diffuse and Characteristic Distribution Total Solar Radiation (1960) stated that, beam radiation, reflecting radiation from the ground and the diffuse radiation on any collector panel can be considered as the total solar radiation on a tilted surface [10][11]. The equational representation can be calculated as per the rate of hourly basis solar radiation of every type on a tilted collector panel[12].

$$I_T = I_B R_B + I_D \left(\frac{1+cos\beta}{2}\right) + I_R\left(\frac{1-cos\beta}{2}\right) \text{----------(11)}$$

$I_T$= Total irradiance angle
$I_B$= Beam radiance
$I_D$= Diffusion irradiance
$I_R$ = Earth reflected radiation

This particular model has been implemented only in USA and Canada where the researchers found it useful for only in cloudiness environment [27].

### 2.3.3.2. ASHRAE Modifications

This specific modified model was developed by Threlkeld and Jordan (1958) titled as American Society of Heating, Refrigerating, and Air Conditioning Engineers (ASHRAE) Clear Day Solar Flux Model, suitable for the dusty atmosphere. This isotropic diffuse model has introduced and declared the value of 3 factor named as apparent extraterrestrial flux generated due to irradiance of sun (A), Dimensionless factor (K) also knows as the optical death and the sky diffuse factor (C) [9].

On a solar year, only half of the solar irradiance emitted by the sun hits the atmosphere of earth and during this process the direct or beam radiation ($I_{BC}$), Diffuse radiation ($I_{DC}$), and reflected irradiance ($I_{RC}$) is equal to the Solar radiation striking a Collector ($I_C$).

$$I_C = I_{BC} + I_{DC} + I_{RC} \text{ ----------(12)}$$

Collector solar radiation ($I_C$) is expressed by $W/m^2$, so does the beam radiance, reflected radiance and diffuse radiance.

.

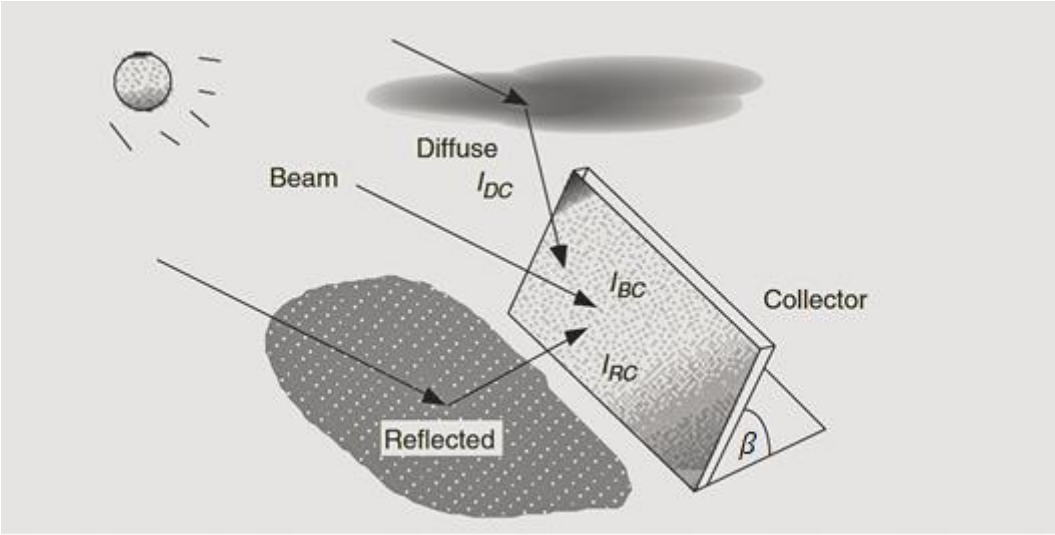


*Figure 5: Irradiance map*

## 2.3.4. Solar Calculation

### 2.3.4.1. Beam solar irradiance

Beam solar irradiance can be expressed as the amount of energy that has to travel through the atmosphere which is easy to be calculated though the other factor of the atmosphere as dust, cloud, pollution level and the humidity of the weather varies from place to place. To calculate the value of beam solar irradiance, a set of equation is well established [13],

$$I_B = Ae^{-km} \text{----------(13)}$$

Equations stated above, $I_B$ is the normal rays reaching to the earth surface, A is the apparent extraterrestrial flux lost in space.

$$A = 1160 + 75\sin[\tfrac{360}{365}(n - 275)] \text{----------(14)}$$

Optical death termed as the dimensionless factor ($K$)

$$K = 0.174 + 0.035\sin[\tfrac{360}{365}(n - 100)] \text{----------(15)}$$

and the air mass ratio ($m$)

$$\text{Air mass ratio } m = \frac{1}{sin\alpha_s} \text{----------(16)}$$

Total solar beam irradiance $I_{BC}$, can be calculated from the value of normal ray irradiation $I_B$.

$$I_{BC} = I_B cos\theta \text{----------(17)}$$

Surface tilt ($\beta$) termed as to demonstrate the tilt angle of the panel created with the horizontal surface axis and the system axis tilt ($\beta_a$) is defined as the function of the system axis tilt [14]

$$\text{Surface tilt, } \beta = cos^{-1}(cosHcos\beta_a) \text{----------(18)}$$

Surface azimuth has a compact relationship with the axis azimuth, as it varies with the “Hour angle (H)”. Surface azimuth,

$$\gamma_s = sin^{-1}[\frac{sinH}{sin\beta}], \text{ ---------- (19)} \qquad \text{For } \beta \neq 0, -90° \leq H \leq +90°$$

Now, the solar azimuth angle (γ) is illustrated as the product of the declination angle ($\delta$) and the Hour angle divided by the surface tilt ($\beta$)

$$sin\gamma = \frac{cos\delta cosH}{cos\alpha_s} \text{---------- (20)}$$

Moreover, altitude angle, surface azimuth, solar azimuth and the angle of the surface tilt associated within this system is calculated to determine the incident angle ($\theta$) of the sun [13]. To be precise, incident angle is the normal ray angle on the photovoltaic panel face and the solar beam irradiance ($I_{BC}$).

$$cos\theta = cos\alpha_s \cos(\gamma - \gamma_s)\, sin\beta + \sin\alpha_s \cos\beta \text{---------- (21)}$$

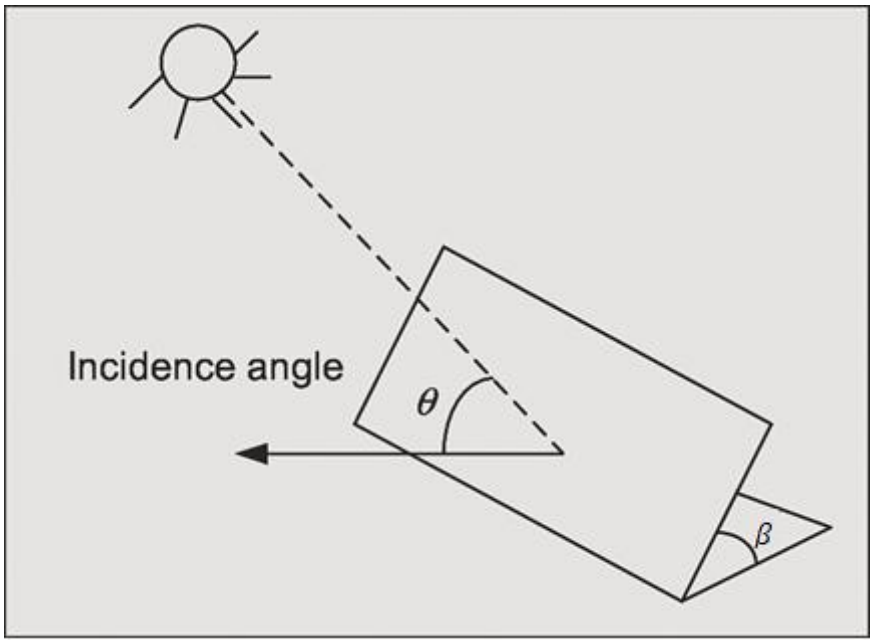


*Figure 6: Incidence angle*

#### 2.3.4.2. View factor

View factor (*v.f)* of the collector to the sky determines the rate of diffuse irradiation on the collector panel within our solar panel system [15]. While considering the view factor to sky of a system, shaded ground *v.f* and non-shaded ground *v.f* along with *v.f* of surface to sky should be summed up to 1.

Front side panel view factor

For front side of the panel, reflection factors are negligible in our system, but the diffusion view factor also termed as the view factor of surface to sky which determines the active view factor.

Diffusion view factor(front), $F_{Vsky} = \frac{1+cos\beta}{2}$ ---------- (22)

Rear side view factor

Rear side diffusion view factor

$$R_{Vsky} = \frac{1-cos\beta}{2} \text{ ---------- (23)}$$

Rear side reflection view factor

The view factor of the rear side of the panel is consists of shaded ground ($R_{Vs}$) and non-shaded ground view factor ($R_{Vns}$).

$$R_{Vs} = \frac{H+S-\left[H^2+S^2-2HScos\beta\right]^{1/2}}{2H} \text{ ---------- (24)}$$

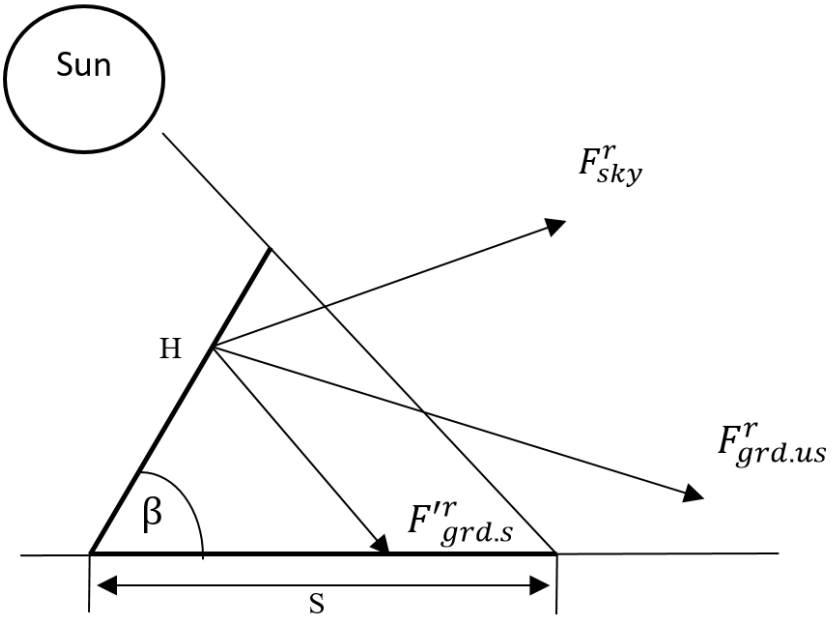


*Figure 7:view factor of shaded ground[15]*

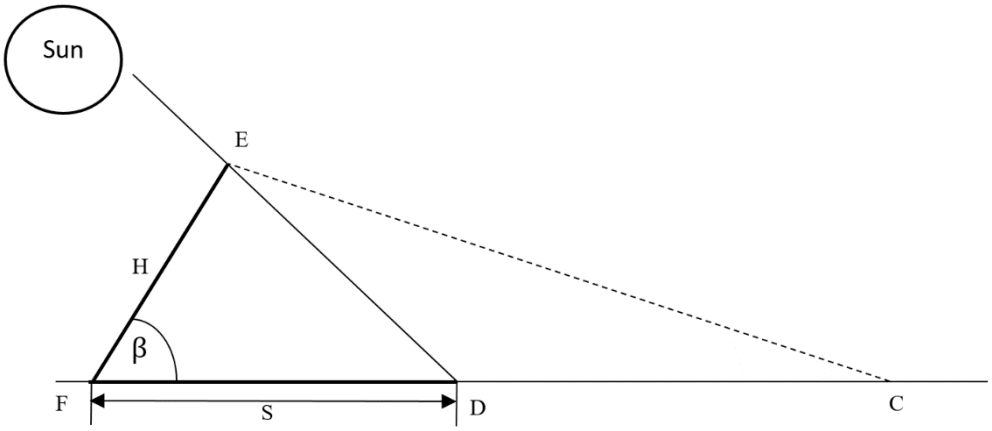


*Figure 8:view factor of non-shaded [15]*

$$R_{Vns} = \frac{Hcos\beta+\left[H^2+S^2-2HScos\beta\right]^{1/2}-S}{2H} \text{---------- (25)}$$

$$Rear\ side\ reflection\ view\ factor = R_{Vs} + R_{Vns} = \frac{1+cos\beta}{2}$$

### 2.3.4.3. Diffuse solar irradiation

The diffuse irradiation is to be calculated as the sky is considered as isotropic and the amount of cloud, dust or brighter day with a clear sky and factors like a cloudy day with rain is expressed as the factor C while calculating the diffuse irradiation of any side of the collector [13]

.

$$I_{DF} = CI_B \frac{1+cos\beta}{2} \text{----------(26)}$$

$$C = 0.095 + 0.04\sin[\frac{360}{365}(n-100)] \text{----------(27)}$$

Similarly, for the rear side of the panel, the diffuse solar irradiation can be expressed as,

$$I_{DR} = CI_B \frac{1-cos\beta}{2} \text{----------(28)}$$

And, the diffusion view factor ($R_{Vsky}$) is used to determine the view factor of rear side diffuse irradiation .

### 2.3.4.4. Reflected solar irradiance

$\boldsymbol{I_{RC}}$, is the available solar irradiation on the collector panel after the reflection from any albedo surface expressed as reflectance.

$$IR_C = \rho I_B(sin\beta + C)\,(\frac{1-cos\beta}{2}) \text{----------(29)}$$

Similarly, we can derive the reflected solar irradiance for the rear side of the collector,

$$IR_{C\rightarrow rear} = \rho I_B(sin\beta + C)\,(\frac{1+cos\beta}{2}) \text{----------(30)}$$

## 2.4.Energy Calculation

### 2.4.1. Multilevel Bifacial Module

Bifacial solar modules expose both front and rear side of the solar module. Total irradiance will be accumulated by the sum of front side and rear side irradiance of the module. Irradiance's nature created by the front side bifacial module are direct and little diffused.

The total energy of the proposed system is the combination of accumulated energy from the total irradiance of three panel modules those are attached in Top, Middle and Bottom position.

$$I_{total} = I_{top} + I_{middle} + I_{bottom} \text{----------(31)}$$

The following expression of total irradiance of a particular bifacial module,

$$I_{tot} = I_{front} + I_{rear} \text{ ----------(32)}$$

Where $I_{front}$ is given by,

$$I_{front} = I_{DF} + I_{BC} \text{----------(33)}$$

And $I_{rear}$ is given by,

$$I_{rear} = I_{DR} + IR_C \text{----------(34)}$$

#### 2.4.1.1. Albedo Factor

Methodological order of calculating the light collection of ground-reflected albedo depends upon the careful consideration of self-shading of the solar modules. Which results into a significant reduction of illumination onto the ground, and consequentially, creates the ground-irradiance on both the sections of a solar module[20].

Albedo factor of a surface is calculated by the formulae,

Albedo factor (ρ) = (Reflected light)/ (Incident light)

#### 2.4.1.2. Effect of Height Boosting:

The Albedo factor is contingent on the height of the panel's positioning. This expression can be described by the following Graph.

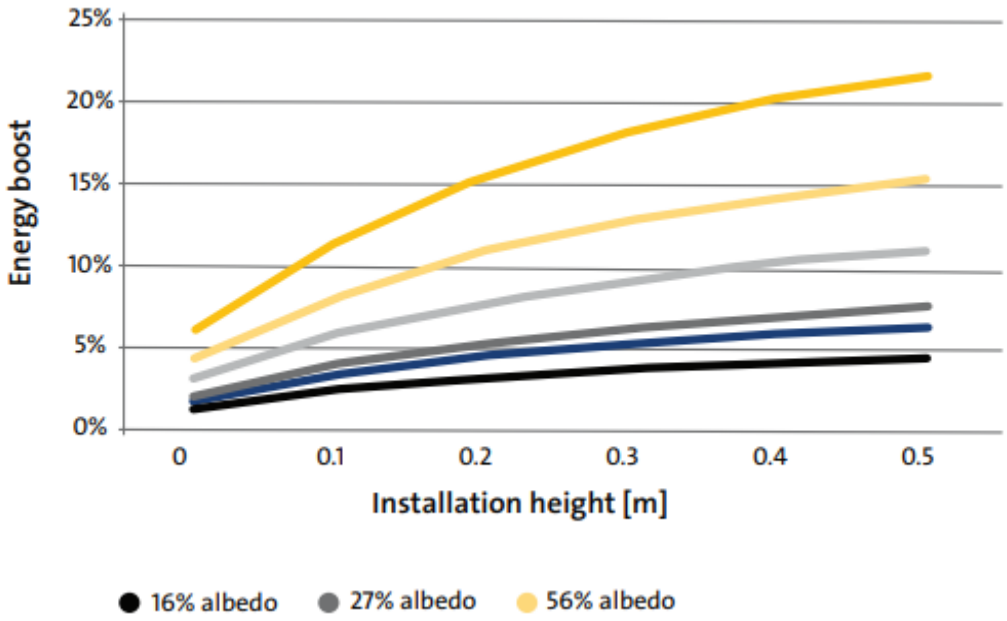


*Figure 9:Energy Boost based on albedo[20]*

If we keep the value of the Albedo factor at 0.4, analyzing the Graph stated above, we gain 10% more reflectance efficiency on the middle panel and 15% more on the top panel compared to the bottom panel of the system.

#### 2.4.1.3. Multitier Panels

Bottom Module: Bottom module follows the general pathway through which we establish the irradiance on the front and rear side of the bifacial module. Hence, the bottom module can be signified via the aggregated value of $I_{front}$ and $I_{rear}$, which can be found from the previously established Equation *(33)* and Equation *(34)*. As a result, we get the same expression of total irradiance. So, total irradiation of the bottom panel is sum of the current of front panel and rear panel.

Top Module: Taking the observation into consideration from (Figure 9), for the top panel $IR_C$ increases at least 15%. Hence, $I_{rear}$ can be calculated by adding $I_{DR}$ and1.15 $IR_C$.
For the front panel, the Equation stays just as same as equation *(33)*
Now, the total irradiance of the top module is calculated using equation *(32).*

Mid Module: The energy calculation of mid panel is slightly different from top panel and bottom panel as the mid panel rotates to vertical position during the time 11am to 1pm. Surface tilt (β) will be 90° during this period of time. As direct beam irradiation can't fall on the surfaces of the module, only diffused and reflected irradiation fall on the both surfaces of the module. As a result, irradiance of the both side of mid panel $I_{front}$ and $I_{rear}$ is equal to front side diffused irradiance, $I_{DF}$. So, the total irradiation of mid panel during 11am to 1pm is $I_{DF}$ on the both front and rear side of the panel.
Outside this period, the irradiation of front side for mid panel is same as top and bottom panel. Only exception is the height boosting effect of the mid panel's rear side is slightly different from the top panel. Using the same graph used to calculate the energy boost of the rear side for top panel, we get the value of energy boost to be 10%. So, for the rear side of mid panel, the value of $I_{rear}$ is given by,

$$I_{rear} = I_{DR} + 1.1IR_C \ldots\ldots\ldots\ldots\ldots \text{(35)}$$

### 2.5.2. Environmental Impact

Cloud effect

Isotropic diffuse module states that all diffuse irradiation is isotropic, meaning the intensity of diffuse irradiation is uniform over the sky dome. Presence of cloud affects the efficiency of solar energy conversion. A significant portion of sun's ray may no longer reach earth's surface due to presence of cloud. Radiation energy by sun collected on a surface can be measured as the solar insolation that can be complied with the cloud density, altitude angle of the sun's location depending on a specific time period. The month wise data throughout the year is collected from [3].

Here we observe in a sunny day the energy harvested is 20% greater than a cloudy day. The related mathematical equation is stated below.

$$E_{sunny} = \int_{T_{SR}}^{Tss} (ISin\alpha + 0.1I)dx \text{----------(36)}$$

$$E_{cloudy} = \int_{T_{SR}}^{Tss} 0.2Idx \text{---------- (37)}$$

$$Proposed\ Multilevel\ Solar\ Panel\ Total\ Energy,$$

$$E_{total} = x * E_{sunny} + y * E_{cloudy} \text{----------(38)}$$

$$x + y = total\ days\ for\ a\ particular\ month$$

| Month | Num. of Sunny days | Num. of cloudy days | Total days |
|---|---|---|---|
| Jan | 28 | 3 | 31 |
| Feb | 23 | 5 | 28 |
| Mar | 25 | 6 | 31 |
| Apr | 20 | 10 | 30 |
| May | 18 | 13 | 31 |
| Jun | 12 | 18 | 30 |
| Jul | 9 | 22 | 31 |
| Aug | 11 | 20 | 31 |
| Sep | 13 | 17 | 30 |
| Oct | 21 | 10 | 31 |
| Nov | 25 | 5 | 30 |
| Dec | 26 | 5 | 31 |
| Total | 231 | 134 | 365 |

*Table 2: Month wise cloudy days data [3]*

### 2.5.3. Electrical energy calculation

Here, to calculate an electrical output of the system for one day, necessary parameters are used to calculate the energy consumption of individual components:
Datasheets of the component as Relay, Actuator, Arduino or servo motors were used to collect the value of these parameters.

Following table represents the rated and supplied current and voltage of the system component.

| | Supply current *mA* | Supply voltage *V* | Operating Time *sec* |
|---|---|---|---|
| Relay | *144* | *5* | *33.32* |
| Actuator | *2000* | *12* | *33.32* |
| Arduino | *40/pin* | *5* | *86400* |
| Servo | *350* | *5* | |

*Table 3:Component rating calculation*

Energy, *E = operating voltage (V) * total output current (I) *Time* ---------- (39)

*Total yearly power consumption of the full system*

*= Daily energy consumption ×Total Number of days in a Year* ----------(40)

*Total output current of Arduino (I) = Number of pins used × Operating current ------ (41)*

Number of used 8 output pins of Arduino for data logger and 7 number of pins are located in control system Arduino [21].

From the equation of *(39)* and *(41)*, Microcontroller energy consumption is 33Wh and data logger system Arduino energy consumption is 38.4Wh.

From the equation *(39)*, relay($E_r$) and Actuator($E_{act}$) Energy consumption is 6.67 mWh and 222 mWh respectively.

Furthermore, in this particular system, we have used 3 servo motors to operate in our system, which consumes 5.25W.

So, the Daily energy consumption by the full system is 76.87 Wh, which derives the total yearly energy consumption = 28.057 KWh.

$$\boldsymbol{Solar\ module\ Electrical\ energy\ output\ per\ day} = Area\ of\ panel \times Efficiency\ of\ panel \times Energy\ Harnessed\ per\ day - Daily\ energy\ consumption\ by\ the\ full\ system \text{ -------(42)}$$

# Chapter 3

# 3. System Design and Simulation

## 3.1 Review on multilevel solar panel

To take advantage of the available space in a more systematic order and make it useful by accumulating more solar energy using PV panels a novel approach was introduced by Rahman et al. in 2013. The proposal directed that a structure of multilevel solar panels will be mounted in an organized way that it will take less space to save the floor area and generate more power. The panels will be furnished with motors, decisively constrained by a microcontroller, which will pivot the panels on a horizontal axis to follow the sun to enhance the power generation for the duration of the day. Later on, in 2017 on the same affair the implementation and verifications experimented and the results showed that a significant amount of increment regarding the energy collection is obtained compared to the conventional single-level fixed panel system.

All the panels are upheld by a solitary SS bar. The SS bar with the heap of panels is mounted on a vertical stand fixed to a substantial iron base in a way so the SS bar can without much of a stretch turn along a flat bend with the activity of the linear actuators. For interfacing, the solar panels with the SS bar three openings were penetrated into the SS bar where iron bars were embedded with little metal rollers so the iron poles can be pivoted easily around the horizontal axis.

Proposed bifacial module based multilevel solar panel system

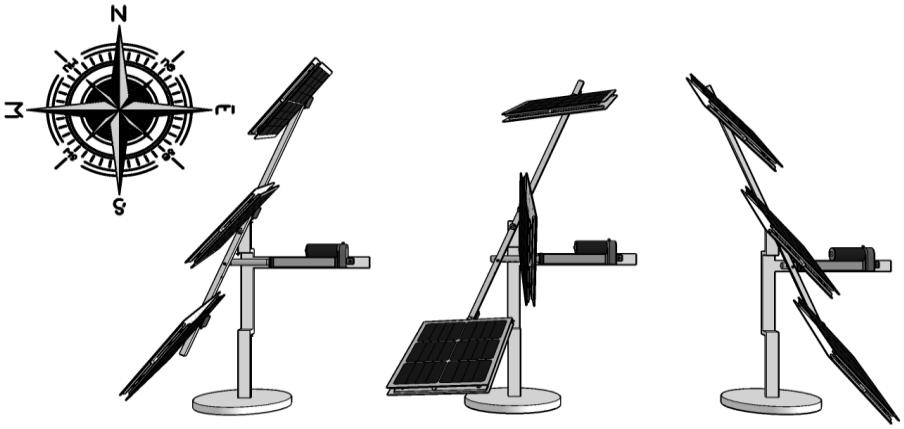


*Figure 10:Proposed bifacial solar panel system*

The proposed bifacial based multilevel solar panel framework is portrayed in Figure 10. The panels are mounted one over another isolated by a fixed distance to limit the floor space and moved on a level plane considerably the board width to stay away from the shading of the lower panels. Every one of the panels will be furnished with a microcontroller-controlled servo motor to follow the sun.

In the proposed framework, each of the three panels is upheld by a solitary SS bar mounted on a vertical remain with a heavyweight iron base so that the SS bar can turn around, appropriately keeping up the framework's solidness. This rotational development along a specific bend way is accomplished with the assistance of an actuator appended to the vertical remain as appeared in Figure 10. A servo motor precisely controlled with a microcontroller to track the sun is equipped with each of the panels.

The panels are facing in the south with an axis tilt of 23.5° with the ground. Following this procedure, all the panels will track the sun for the entire day to get the full exposure of the direct irradiance. However, during the time of 11 am to 1 pm the middle panel will be in a vertical position to avoid shading of the bottom panel and get the diffused irradiance on both sides of the bifacial panels. The top and bottom panels will harness a significant amount of Direct irradiance, Diffused irradiance, and Reflected irradiance, to generate more power and

add more efficiency. With the help of the microcontroller, servo motor the panels will track the sun from the sunrise time and it will keep the same alignment with the sun. The middle panel will be changed to a vertical position for the referred time of the noontime in order to avoid shadows for the bottom panel. Due to the vertical position of the middle panel, the upper-level panel and lower-level panel will get the maximum disclosure of the solar power to get all the direct, diffused, and reflected irradiance but the middle panel will only be energized by the diffused irradiance. After 1 pm all the panels will be aligned with the sun again as the sun moves towards the west side. The core advantage of the system is the height boosting the position of the bifacial panel is the upper and the middle panel receive additional energy due to their position and the bifacial system will get different irradiance for their different heights, to sum up, increased energy.

## 3.2 System design

### 3.2.1 Bifacial Solar Panel Structure

In a single diode and two diode model, Vivek Tamrakar stated that to analyze characteristics of solar cells, electrical equivalent circuits are realized and controlled using simulation software [14]. The best use of any project simulation is to estimate the exact behavior of that specific project under fixed environmental conditions and further in obtaining (I-V) and (P-V) characteristic curves. This research book is written and proposed as to demonstrate a bifacial solar panel system that will harness more energy than a typical solar panel system.

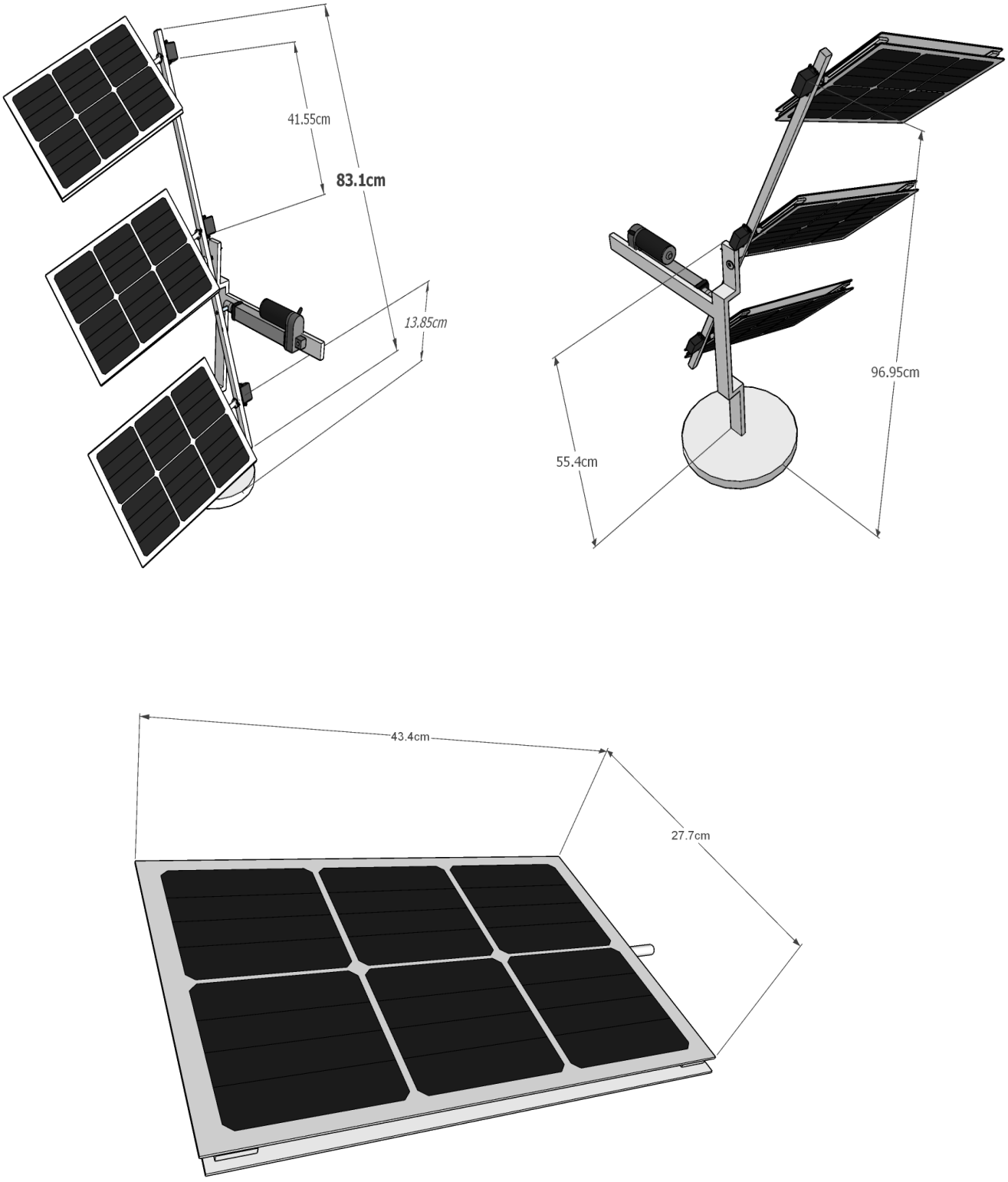


*Figure 11: Multilevel Bifacial Solar Panel  Module*

Figure 11 represented above is the proposed design model of our multilevel bifacial solar panel and the schematic view shows the orientation of panels within the system. In this case, the panels are mounted on top of another and these panels are supported by a single stainless-steel bar which is mounted on the vertical steel connected to the ground with a heavyweight iron base. To maintain the system's ability and proper irradiance during the day the ss bar is mounted in such a way that the panels will rotate freely without blocking the sun rays while the rotational control will be performed by the stroke of an actuator receiving input from a servo motor.

The mention design structure of the multilevel bifacial solar panel system has following measurement to construct:

| | |
|---|---|
| Inter panel separation | 41.55cm |
| Height of the vertical support | 55.4mm |
| Overall height of the system | 96.95cm |
| Supporting Bar length | 83.1cm |
| Overall lateral Dimension | 554*434$mm^2$ |

*Table 4: Structural measurement[17]*

Each solar panel is connected with a servo motor precisely controlled with a microcontroller to track the sun while the initial position of the solar panel will be facing east with and angle of position getting the full exposure of the sun.

During the time of sunrise, all the panels attached to the gliding bar will be facing towards the east, as this enables the panels to become fully exposed and available to absorb the energy fully. As in the design, implications show that the panels are shifted from right to left from the bottom panel to the top panel to get the full exposure.

During the noon, approximately from 11am to 1pm when the sun is directly on the overhead of the panels and the middle panel will be in a vertical position to avoid shading on other two panels. This procedure will allow the sun exposure to directly fall upon the top and bottom panels. This time duration for this process is achieved by the position of the sun for which the lower panels start getting shaded over by the upper panels. This position of the sun is a function

of the inter-panel separation and it will be at a higher altitude in the sky for larger inter panel separation. As per the previous research done on the multilevel solar panel system, provides information that the inter panel separation for this system has to be 1.5 times the panel width as this enables the middle panel to harness a significant amount of energy [17].

### 3.2.2 System Weight calculation

Total Weight Carried by the Servo:

| | |
|---|---|
| Single Solar Panel cell weight | 0.3 kg |

*Table 5: Servo Weight*

Solar Panel Round Bar total weight

| | |
|---|---|
| Solar Panel length | 0.434 m |
| Overall weight of the round bar (radi1) | 0.06944 kg |
| Total Weight | 0.20832 kg |

*Table 6: Solar Panel Round Bar Weight*

Solar Panel Plate total weight

| | |
|---|---|
| Solar Panel Width | 0.272 m |
| Plate Bar thickness | 4.7625 mm |
| Plate Bar Width | 25.4 mm |
| Estimated Weight | 0.9488976 kg/m |
| Total Plate Bar Weight | 3.097 kg |
| 4 Plate Bar Weight | 1.0324 kg |

*Table 7: Solar Panel total Weight*

Total Weight of the Single Panel Module

| | |
|---|---|
| Supporting Bar Length | 0.831 m |
| Estimated Weight | 0.8 kgm |
| Overall Weight of the Gliding Bar | 0.6648 kg |
| Single servo weight | 0.055 kg |
| Total Weight of the 3 Panels | 5.68716 kg |

*Table 8: Total Weight of the Single Panel*

Solar Panel Round Bar total weight = Overall weight of the round bar * 3 --------- (43)

Total Weight Carried by the Servo = (Single Solar Panel cell weight *2) + Solar Panel Round Bar total weight + Solar Panel Plate total weight= 1.84072 kg---------- (44)

Total weight carried by the actuator = Total Weight of the Single Panel Module * 3 + Overall Weight of the Gliding Bar = 6.35196 kg---------- (45)

### 3.2.3 Finding Torque to Rotate

Here, m= total weight carried by the servo (kg) and 'R' = Solar Panel Width /4 (m)

$$Torque\ (\tau) = fRsin\theta \text{ ---------- (46)}$$

$$= \frac{mgR}{2} \quad ; \quad [\text{When } \theta = 90°]$$

As per the calculation based on equation no. (*46*), necessary torque will be 0.624Nm to rotate.

### 3.2.4 System Actuator stroke calculation

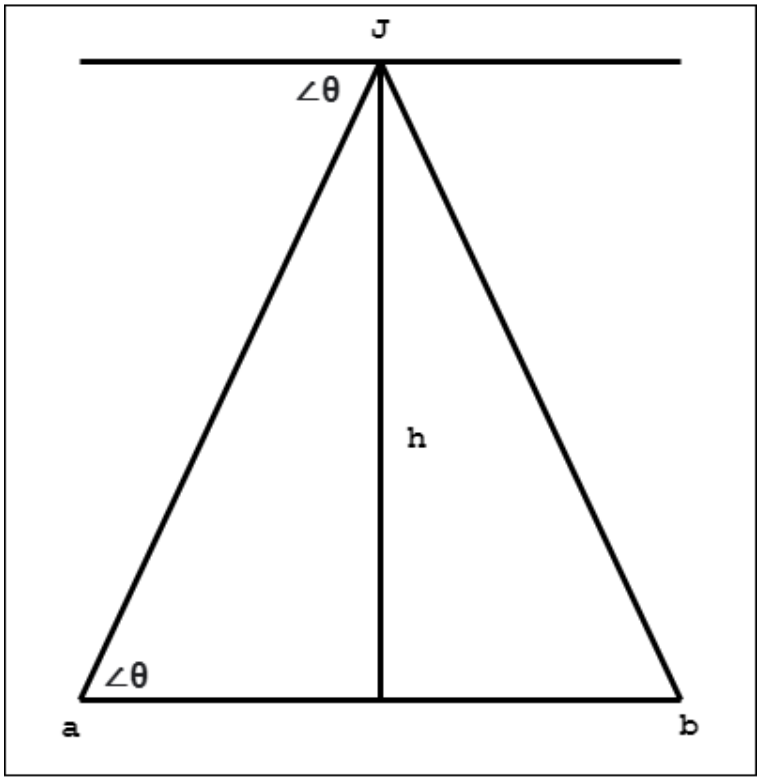


To avoid shading on the middle panel because of the top panel and to the bottom panel, 1.5 times width of distance is maintained to build the structure. But the actuator which moves the panel back and forth. Here θ= 67.5°, created with the gliding bar and the vertical panel. Height of the vertical bar (from actuator connected point to the center of the gliding bar) = 12.07cm.

*Figure 12: System actuator stroke*

$$tan(\theta) = \left(\frac{h}{\text{ab}}\right)*2. \quad \text{---------- (47)}$$

So, actuator stroke length ab = 10cm can be calculated from the above equation.

Within the system, required stroke length of the actuator ab = 100mm. and that is sufficient enough to rotate the gliding panel along with the position of the sun.

## 3.3 System Components

### 3.3.1. Servo motor

The Servo motor has the capability of rotating very precisely at the given angle. This type of motor consists of a circuit system that provides feedback on the current position of the rotor. This is a closed-loop feedback system. Here the device is controlled by a feedback signal generated by comparing the output signal and reference input signal. The main component of servo motors is a DC motor and a feedback circuit.

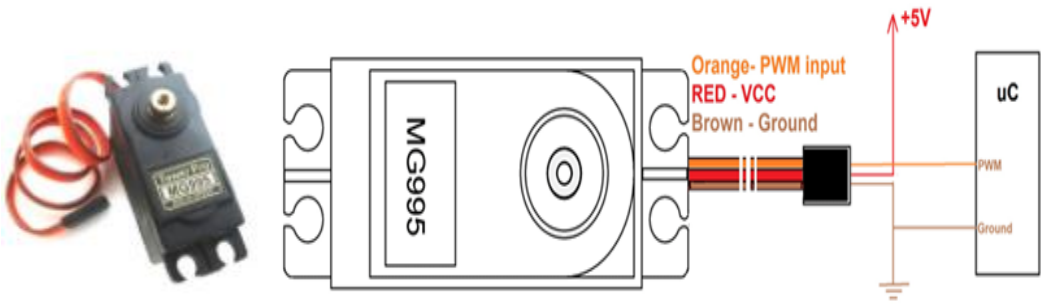


*Figure 13 Servo motor controlling system*

### 3.3.2. RTC

A real-time clock (RTC) is an integrated circuit that keeps an updated track of the current time. To be precise, RTC counts hours, minutes, seconds, months, days and even years with facilities like automatically adjusted for months with fewer than 31 days or even a leap year. To keep tracking the time even when the system power fails, RTCs are designed to operate and consuming ultra-lower power to operate is one of its best features.

Maintaining the clock of an RTC is done by counting its clock by counting the cycles of an oscillator – usually an external 32.768 kHz crystal oscillator circuit, capacitor-based oscillator or an embedded quartz crystal. Different kind of several RTCs can identify transitions and measure the periodic time of any input signal to measure the time.

The simple serial interface helps it to communicate simultaneously with a microcontroller [22]. The clock operates in either the 24-hour or 12-hour format with an AM/PM indicator. Data can be transferred by 1 byte or 31 bytes in a burst mode to and from the clock/ram: CE, input-output data, serial clock

- Completely manages all timekeeping functions
- Simple serial port Interfaces to the most microcontroller
- Simple 3-wire interface
- Low power operation extends battery backup
- 8 pin DIP and * pin SO minimizes required space
- 2v to 5.5 v full operation

### 3.3.3. Actuator

An actuator is one sort of mechanical arm that performs a significant part in controlling and moving a structure. It ordinarily works by the impact of an energy source, for instance, electric current, hydraulic fluid pressure, or pneumatic pressure, and changing over the information energy into movement. An actuator is a gadget by which a control framework acts relying upon the encompassing. The control framework can be basic. It very well may be programming based, a human, or some other info. There are various classifications of actuators. Hydraulic actuators, Pneumatic actuators, Electric Linear actuator and so on. In our multilevel solar

powered board, we have utilized a direct actuator due to the way that movement is made in an orderly fashion in the straight actuator, contrasted with the roundabout movement of an ordinary electric engine.

Each kind of actuator all shows both great and alternate qualities that we should weigh while deciding the correct one for their application project. By figuring out what attributes are non-debatable from the beginning, we will start to preclude certain actuators dependent on these necessities. In the event that it narrows down to two explicit actuators both ready to effectively take care of the work vital, we might need to consider the whole expense of the framework: this incorporates the initial investment, maintenance, and repair fees, just as the expense of potential dangers we could match with each movement segment framework.

| **Characteristics** | **Pneumatic** | **Hydraulic** | **Electric Linear** |
|---|---|---|---|
| Peak power | High | Very high | High |
| Control | Simple valves | User dependent | Flexibility of motion control capabilities with electronic controller [23] |
| Speed | Very high speeds | Moderate speeds [23] | Moderate speeds |
| Load ratings | High load ratings | Extremely high load ratings | Can be high depending on the speed and positioning desired |
| Lifetime | Moderate lifetime | With proper maintenance, it can last a long lifetime | With proper maintenance, it can last a long lifetime |
| Acceleration | Very high | Very high | Moderate |

| | | | |
|---|---|---|---|
| Environmental | High noise levels | Hydraulic fluid leaks and disposal | Minimal |
| Efficiency | Low | Low | High |
| Maintenance | High amount of maintenance | High-user maintenance throughout the life of the system | Close to no maintenance except for when replacements are necessary |
| Operating cost | Moderate cost | High cost | Low cost |

*Table 9: Actuator Comparison[23]*

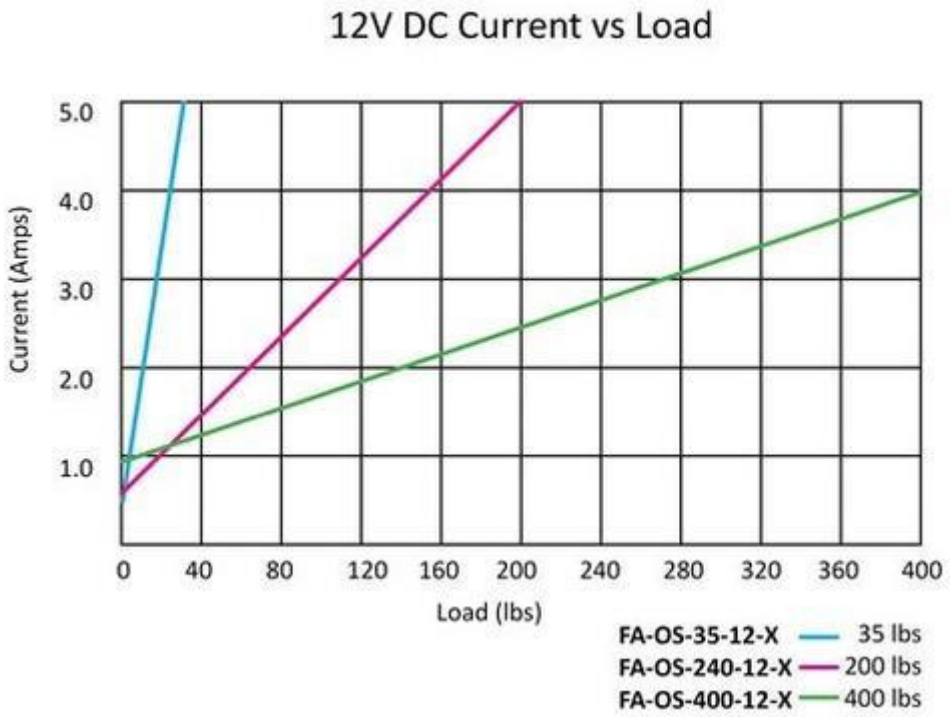


*Figure 14:Actuator Current vs Load [24]*

### 3.3.4. Relay Module

A relay is an electro-mechanical switch. A magnetic field is created during current passing through the coil of the relay that pulls in a switch and changes the switch contacts. The coil current can be on or off so relays have two switch positions and they are twofold toss (changeover) switches. An electrical circuit is controlled by the relay by opening and closing contacts on other circuits. The relay's switch associations are typically marked COM/POLE (Common), NC (Normally Closed), and NO (Normally Open). The working voltage of the relay is 5V/12.

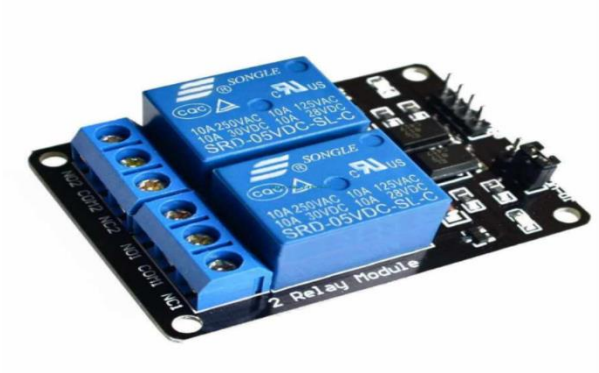


*Figure 15:Dual channel relay module*

Two pins A and B are two finishes of a coil that are kept inside the relay. The coil is twisted on a little bar that gets polarized at whatever point current goes through it.COM/POLE is constantly associated with NC (Normally associated) pin. As current is gone through coil A, B, the post gets associated with the NO (Normally Open) pin of the relay. In our framework, we have worked with a 2-relay module.

This is an opto-coupled relay board having two inputs each for one channel. The relay inputs are at the base right-hand side of the board while the relay outputs are located at the top side of the board. The center position of each relay is the common point, the connection to its left is the normally closed (NC) contact, while the connection to the right is the normally open (NO) contact [25].

In order to determine the direction of actuator piston travel two relays are utilized to flip the positive and negative capacity. 12V force supply is given to the NC pin and the NO pin is grounded when the actuator is idle. At the point when the NC pin is grounded and the NO pin

is given 12V the relay switch is pressed and the code peruses the current position and afterward figures out which bearing to drive the actuator piston to arrive at the objective position. When the objective position is reached, it shuts off the power of the motor [26].

### 3.3.5. Data logger

To collect the output current and voltage from the three panels of the multilevel solar system and fixed panel, a six-channel (3 for current and 3 for voltage) data logger was used. As per the theoretical and practical implementation of the previous studies suggest that the position of the top and bottom level of the solar panel remains the same throughout the day, so the output current from both the panels is fed into a single current channel. Two more separate current channels are used to collect the output current of the middle panel. A 40 AH 12V lead-acid battery has been used as the load of the system. To prevent the reverse current flow from the battery to panel in case of deficiency of sunlight, Schottky diodes are put in series with the each of the panels.

## 3.4 System Operation

### 3.4.1. Software implementation

For our proposed system, Arduino IDE, version 1.8.5 is used as the code editor and compiler. This is an open-source code editor and compiler for various microcontroller board including all Arduino boards, Node MCUs, and others. The vast library that is offered by this software is very useful and time efficient. For our project, we have to use several library including servo's RTC library, SD card library etc. after writing the code and compiling the we used USB com port to transfer the compiled code to Arduino board. For simulation, a .HEX file was generated and added to the simulation software directory.

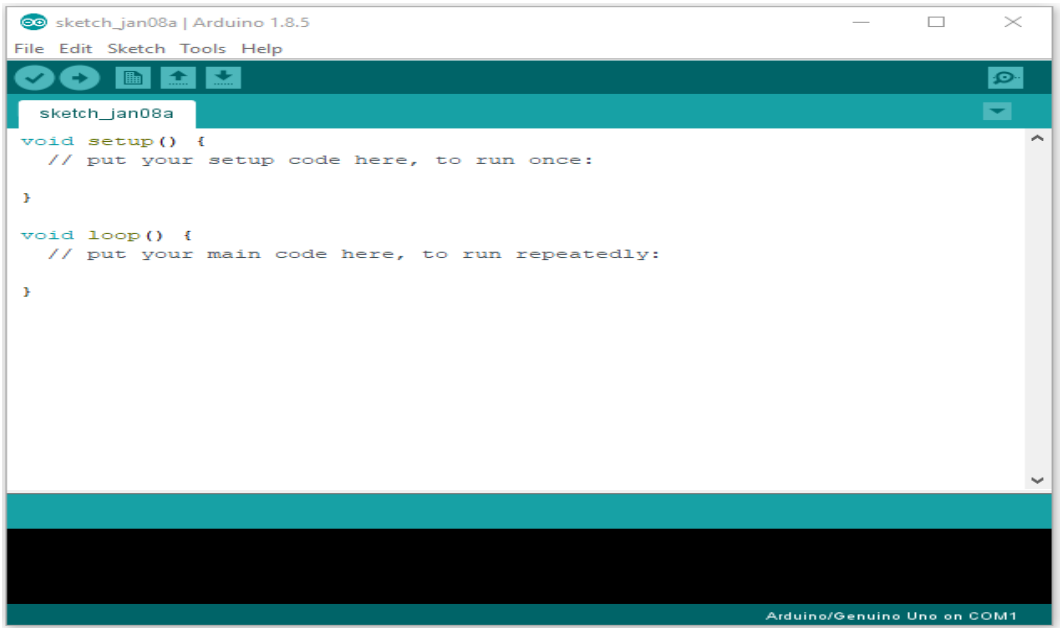


*Figure 16: Arduino User Interface*

The simulation of the proposed system was done in proteus 8.6. Proteus is a proprietary software used to design and simulate electric design automation. The software is mainly used for creating schematics and circuit boards. Proteus comes with a wide range of components library however; it does not come with some key components we used to design our system. In our system design RTC and Arduino plugin and library were used.

## Control system operation

For time measurement RTC DS1307 breakout board is used. The main brain of the system is Arduino UNO microcontroller, shown in Figure 17. Control system operation controlled by the Arduino is connected with the servo motor of the system which has a rotational range of 180°. Function of the operating relay within the system is to control the actuator stroke. Following figure does not contain the actuator model rather the active DC motor was used.

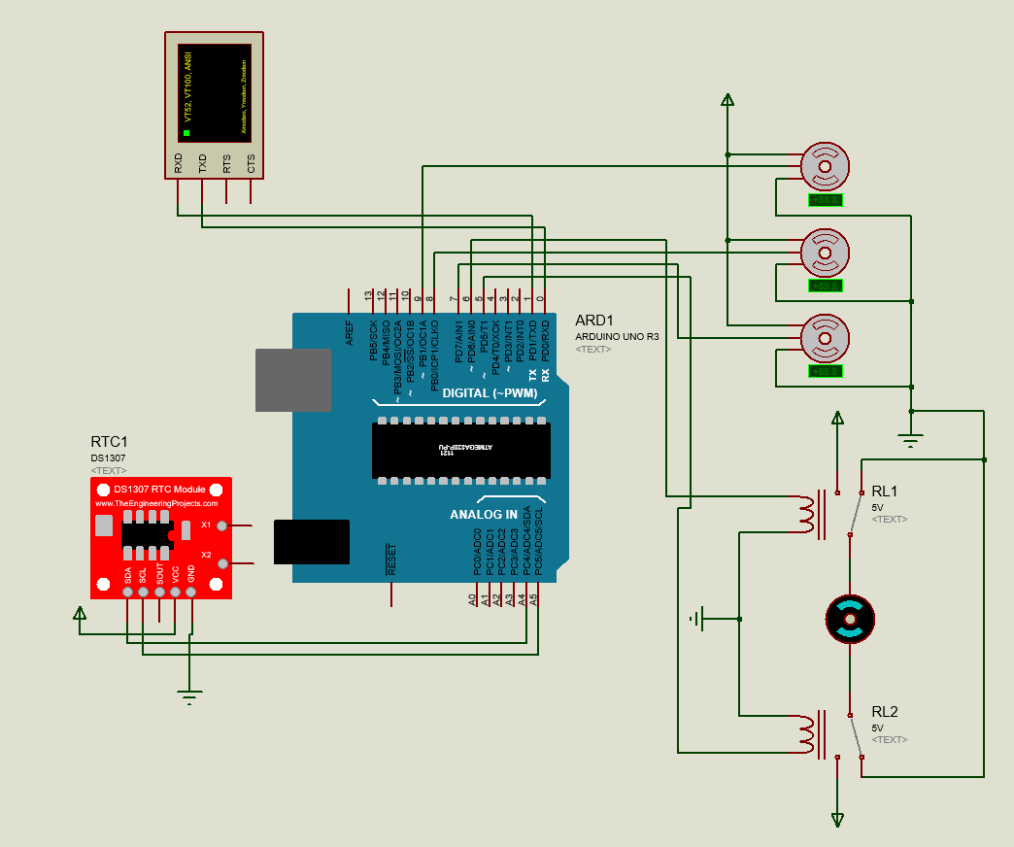


*Figure 17:Circuit diagram of the control system*

Control system flowchart

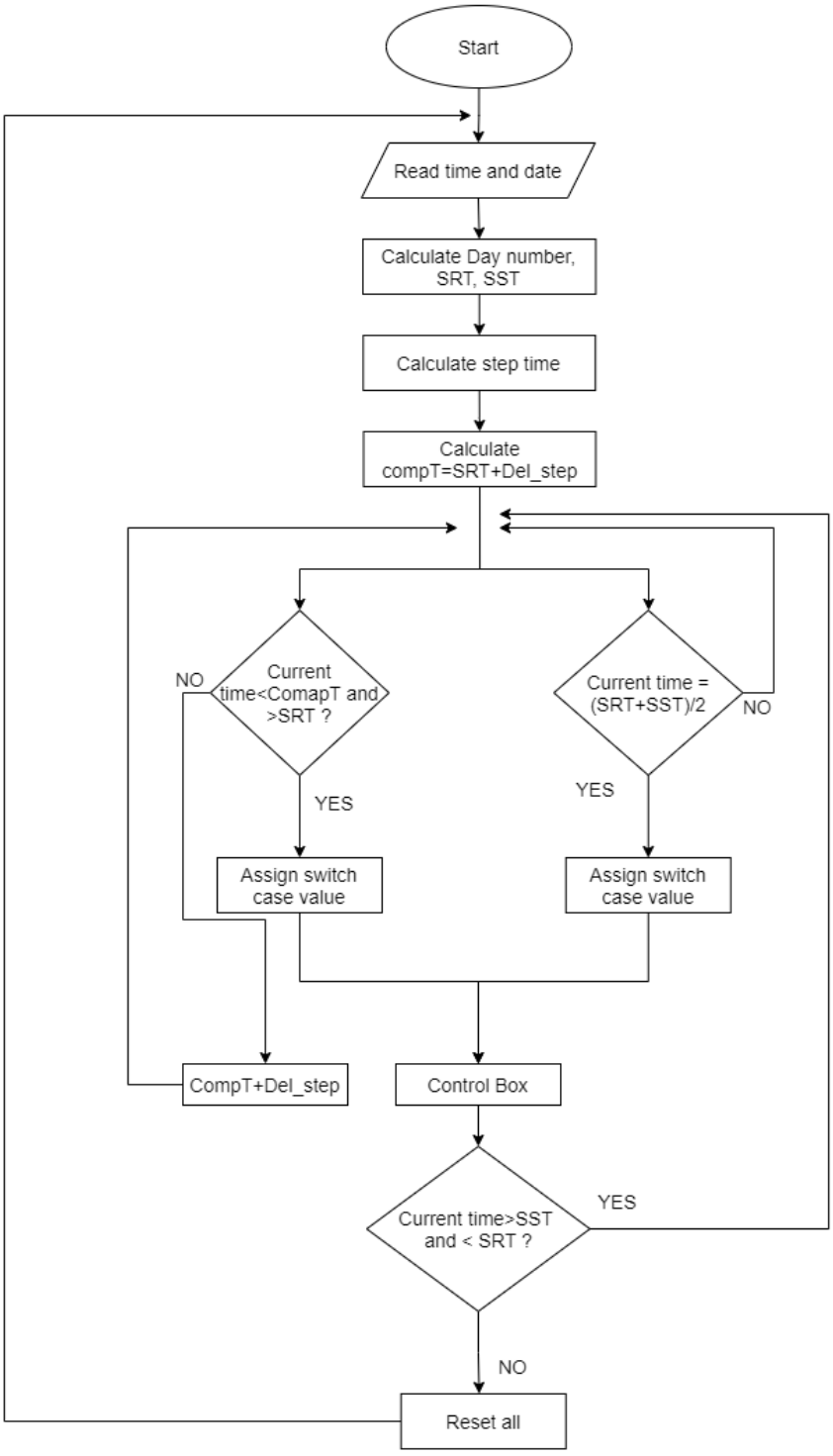

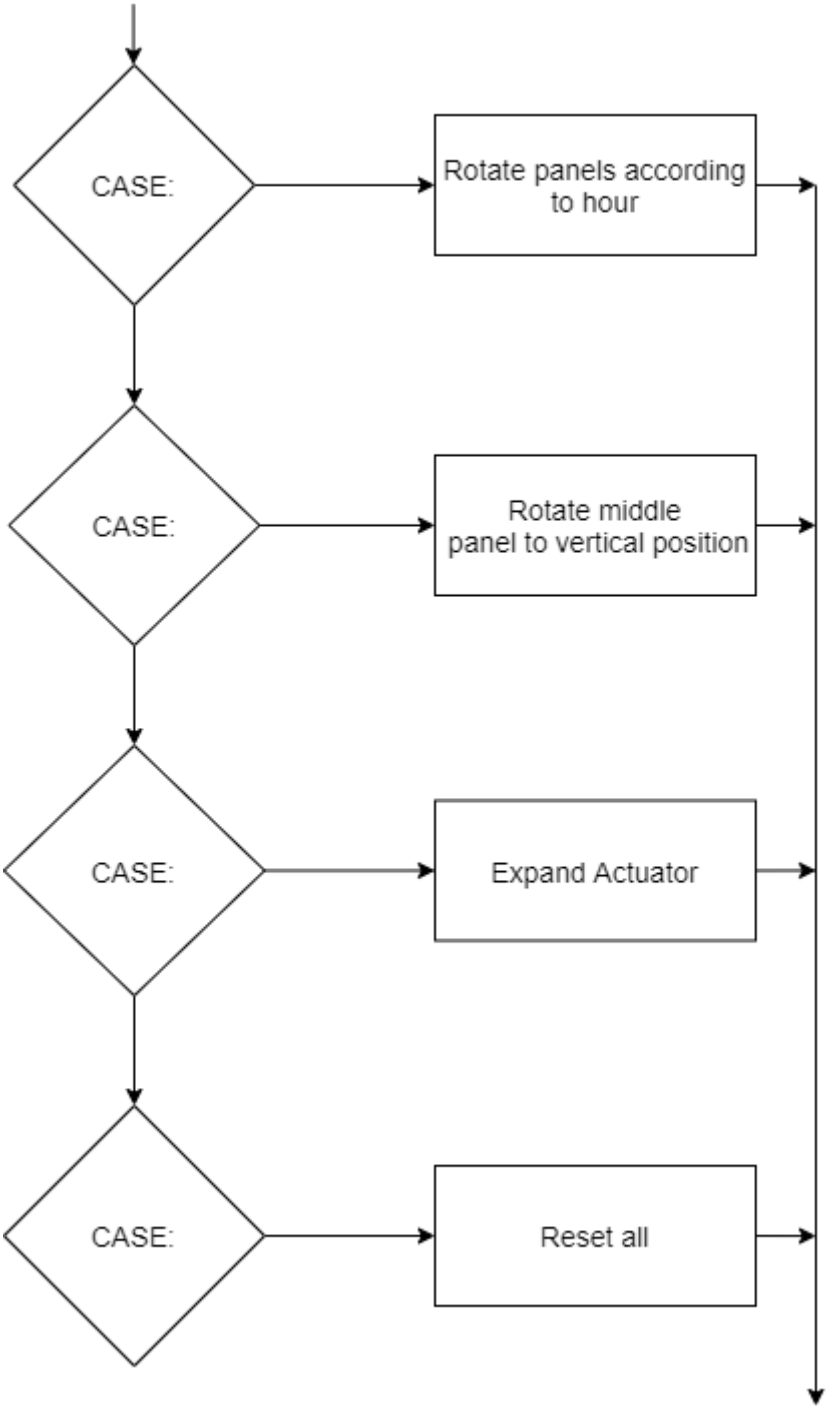


*Figure 18:Control System Flow Chart*

Control system Algorithm

**Step 1:** Reading date and time from RTC module.

**Step 2:** Calculate Day number, sunrise time, sunset time.

**Step 3:** calculate step duration by dividing the sun hour by 12.

**Step 4:** CompT is calculated by SRT+Step time.

**Step 5:** compares if the current time lies between the sunrise time and compT. If the statement is true, then a switch case value X is assigned. If the statement is false, then new CompT is calculated by adding step time with previous CompT.

**Step 6:** Checks if the current time is equal to Noon. If the statement is true then X value is assigned.

**Step 7:** Execute switch case

**Step 8:** check current time is > sunset time or < Sunrise time. If true reset everything and return to step 1. If false return to step 5

Control system simulation

The following figures listed from Figure no. *19-22* shows the steps of servo motor on three different time period during a particular day. Such as, the figure 19 demonstrates the local sunset and current time on the right corner window of Virtual terminal along with the servo position which ultimately rotates the panel likewise.

For simulation purpose, State 2, State 6 and state 10 of a servo position is shown below.

**State 2:**

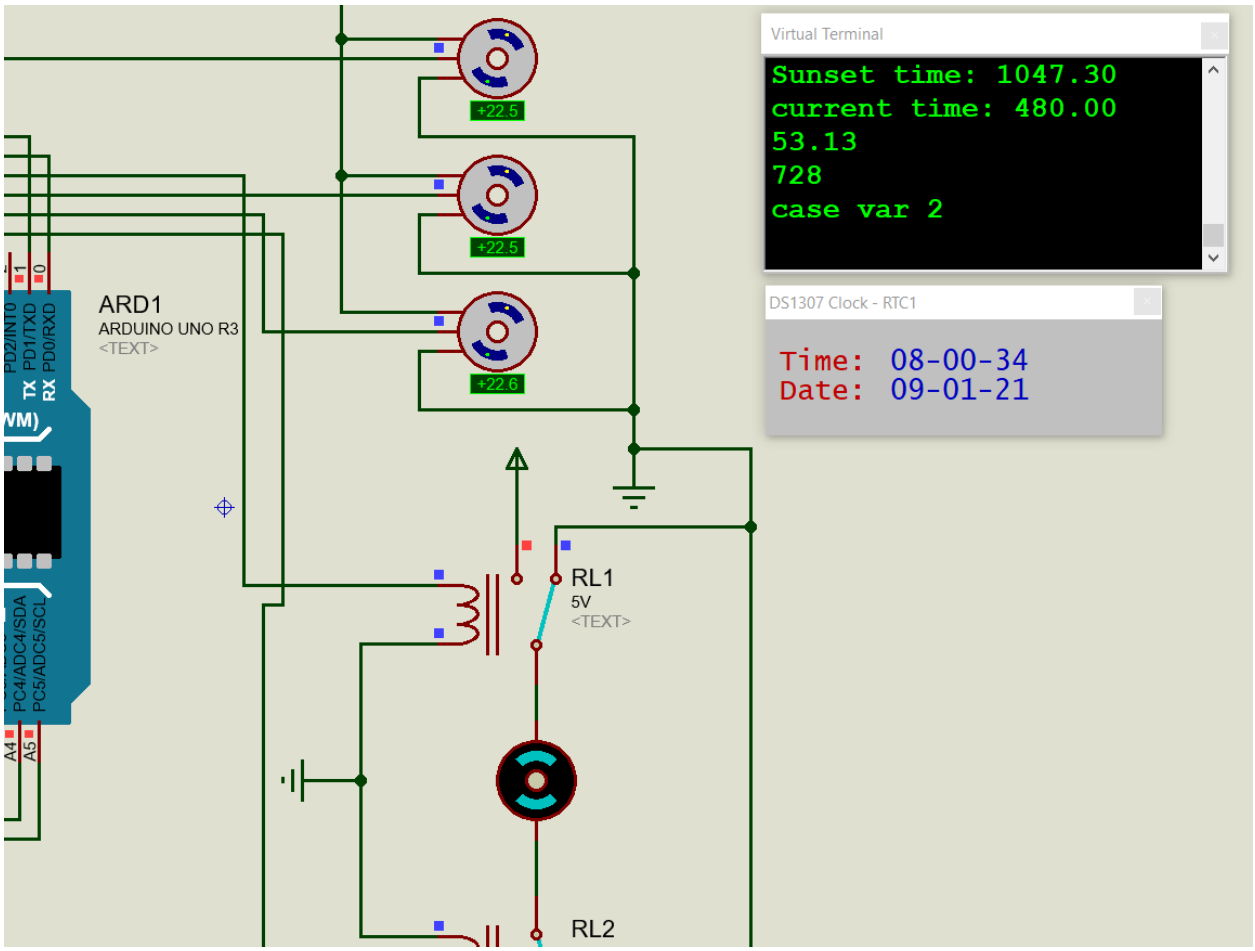


*Figure 19 Morning state of the simulation*

Here, **State 2** starts from 8am. The position of all three servo is at 22.5˚ to the east. Servo position will stay at this position till next state.

**State 6:**

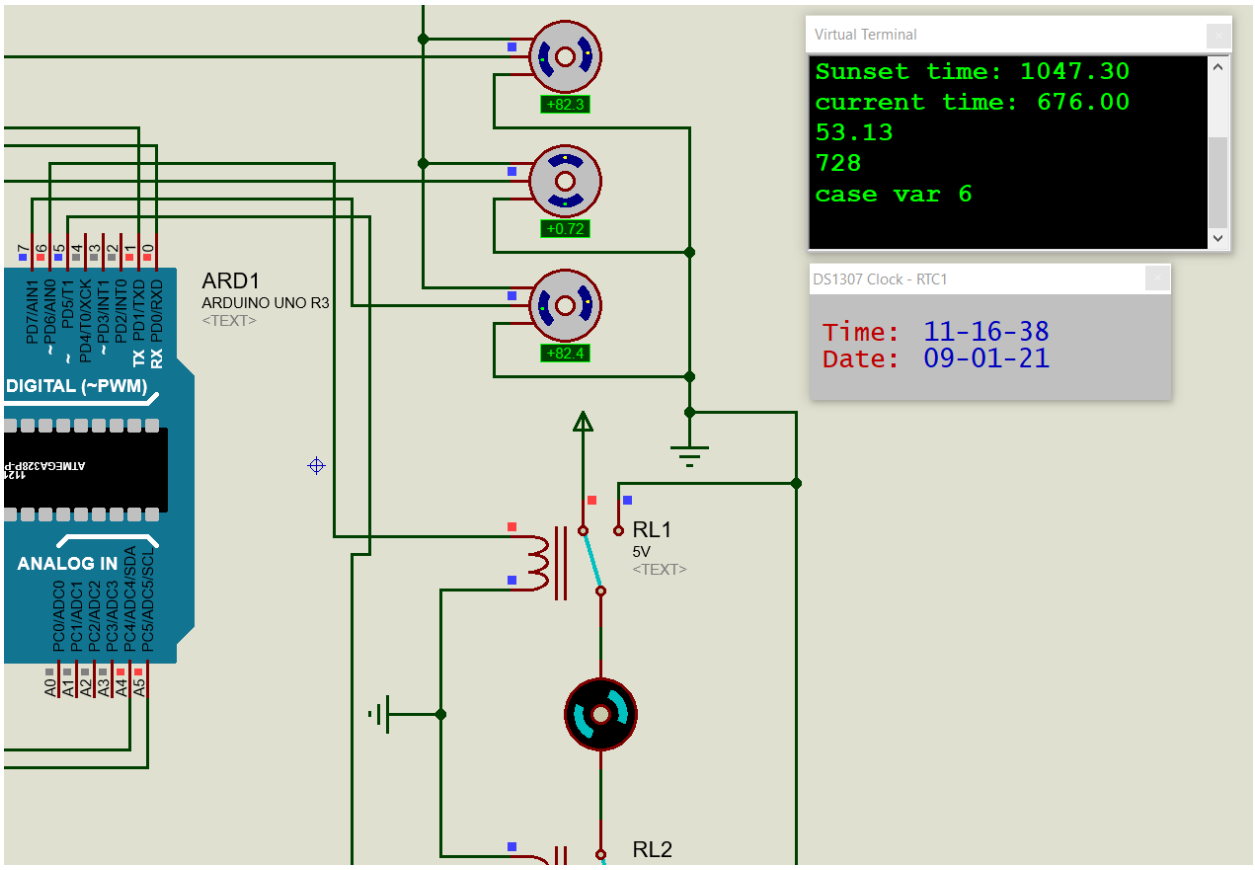


*Figure 20:Noon state of the simulation*

Here, **state 6** starts from 11:16am. Top and bottom servo position is at 82.5° and the middle servo is at 0° position. The actuator expands 100mm. The linear movement of the actuator tilts the gliding bar to the west.

**State 10:**

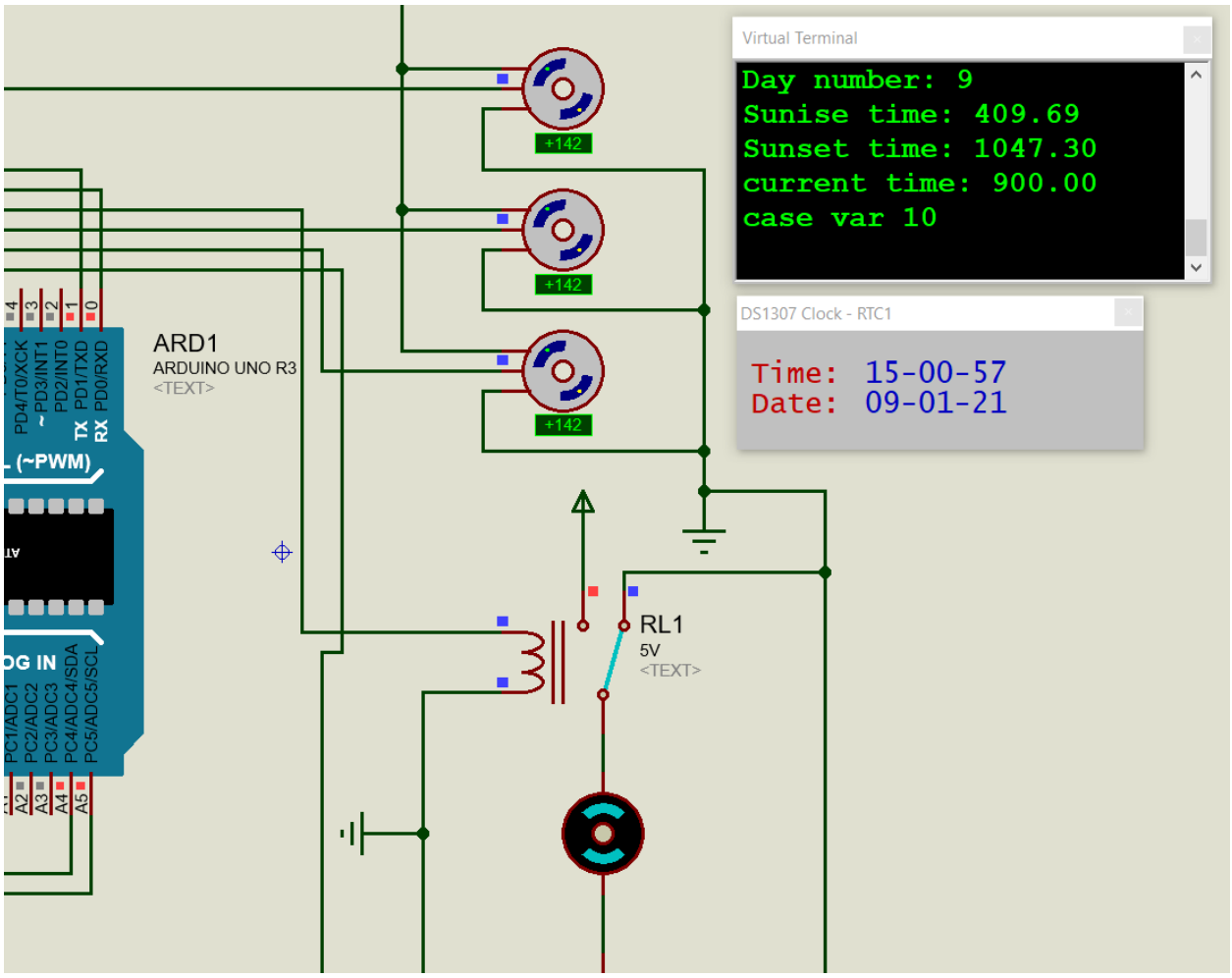


*Figure 21:Evening state of the simulation*

Here, at 3pm all panels are aligned with the same angle of 142.5° . Gliding bar stays tilted to the west.

Data logger flow chart

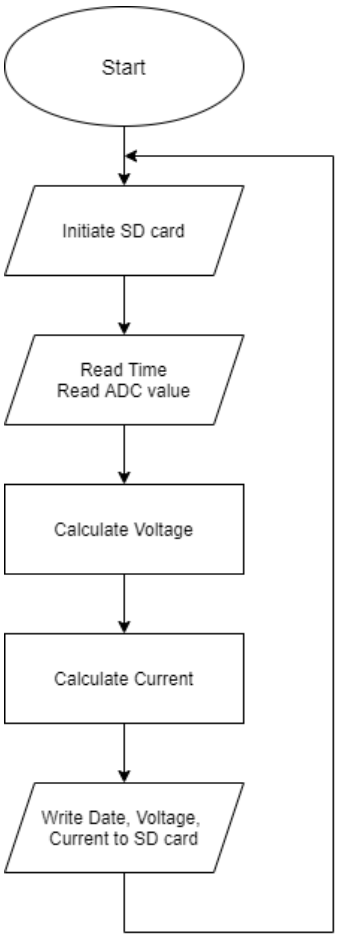


*Figure 22:Data logger*

Data logger algorithm

**Step 1:** initiate SD card

First, the microcontroller initiates the SD card and checks for the data.txt file. If the file is available the program proceeds to the next step.

**Step 2:** read date and time

The microcontroller then reads time and date from the RTC module.

**Step 3:** Read ADC value

Analog pins A0, A1, A2 are connected to the voltage divider network. These pins read voltages from the network and store in ADC value1, 2 and 3.

**Step 4:** convert ADC value to voltage and current

The microcontroller then converts ADC values to voltage. The ADC values vary from 0 to 1023. So, to convert the voltage to a 12v scale the following equation is used

Then the voltage-current is measured using ohm's law.

**Step 5:** write the date, time on the SD card

The microcontroller then opens the file from the SD card and writes the current date and time and the value of voltage and current.

**Step 6:** close file

**Step 7:** Return to step 2.

Datalogger simulation:

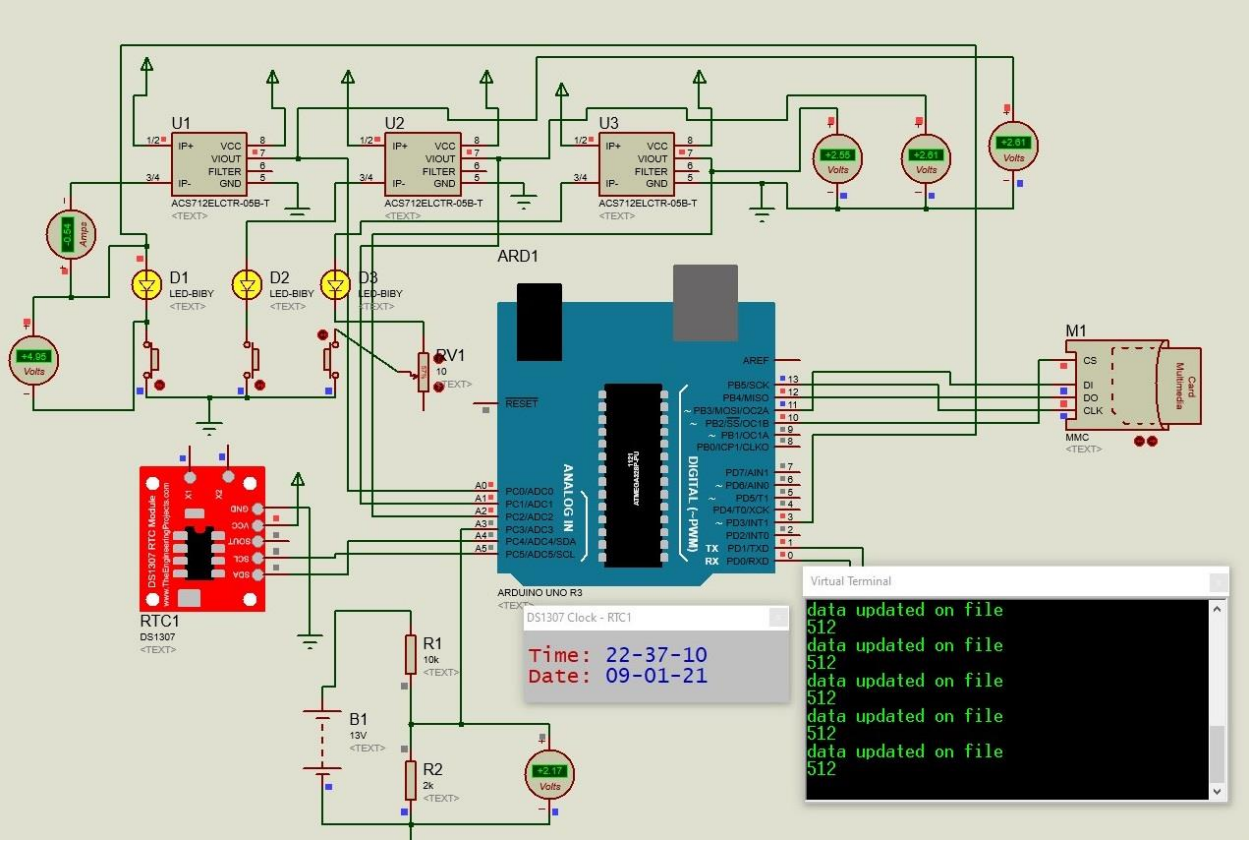


*Figure 23:Data logger simulation*

Here, data logger is collecting data from voltage sensors connected to the analog pins of the Arduino. After converting the sensor values into voltage and current value, the data stored to the SD card according to time and date. These data can be collected from the SD card.

### 3.4.2 Control system

3.4.2.1 Power distribution block diagram:

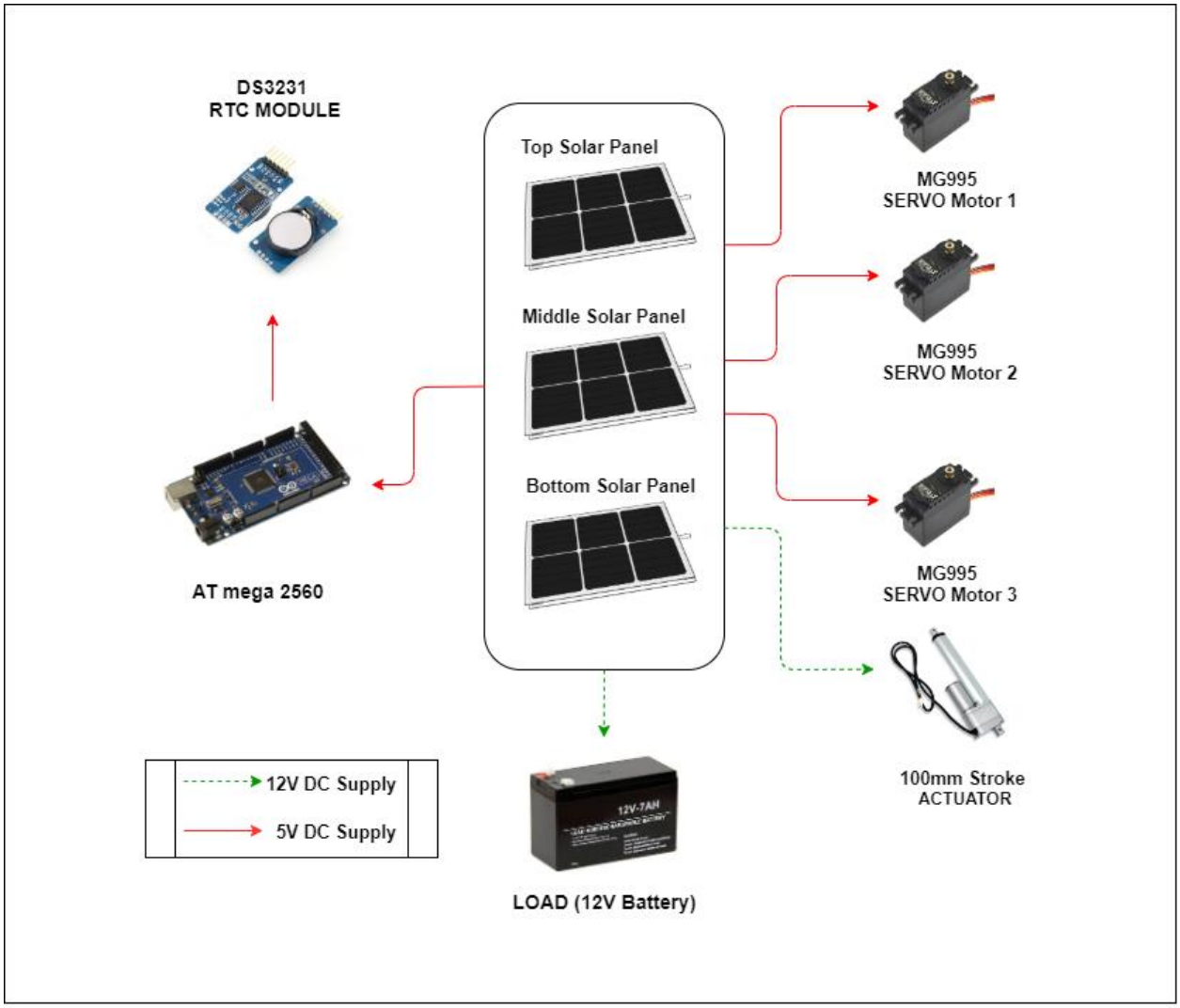


*Figure 24:Power System Block Diagram*

The figure 24 upholds the pictionary of the multilevel bifacial solar panel system with a clear vision of required components. In the framework, three solar oriented panel boards are scaled on a stack that changes energy from the sun into electrical energy. The revolution of the solar panel boards and therefore the direct development of the actuator is constrained by a control circuit that peruses the time from the Real-Time Clock as information. A battery gathers the

electrical energy from where the load draws fundamental power. Here, the three panels are mounted above one another, rotated by the stroke of a 100 mm, stroke actuator controlled by three several servo motors. The voltages and currents created by the boards are likewise gone through the voltage and current sensors of a predesigned information logger for recording those qualities in a memory card. The pre-attached data logger stores the rating of output voltage and current by storing in the memory card for further evaluation and experimental use. The whole system is managed and operated by the microcontroller model atmega2560. This project design implementation represents the simulation approval of working and operating a bifacial solar model with a better rate of efficiency.

3.4.2.2. Signal flow diagram

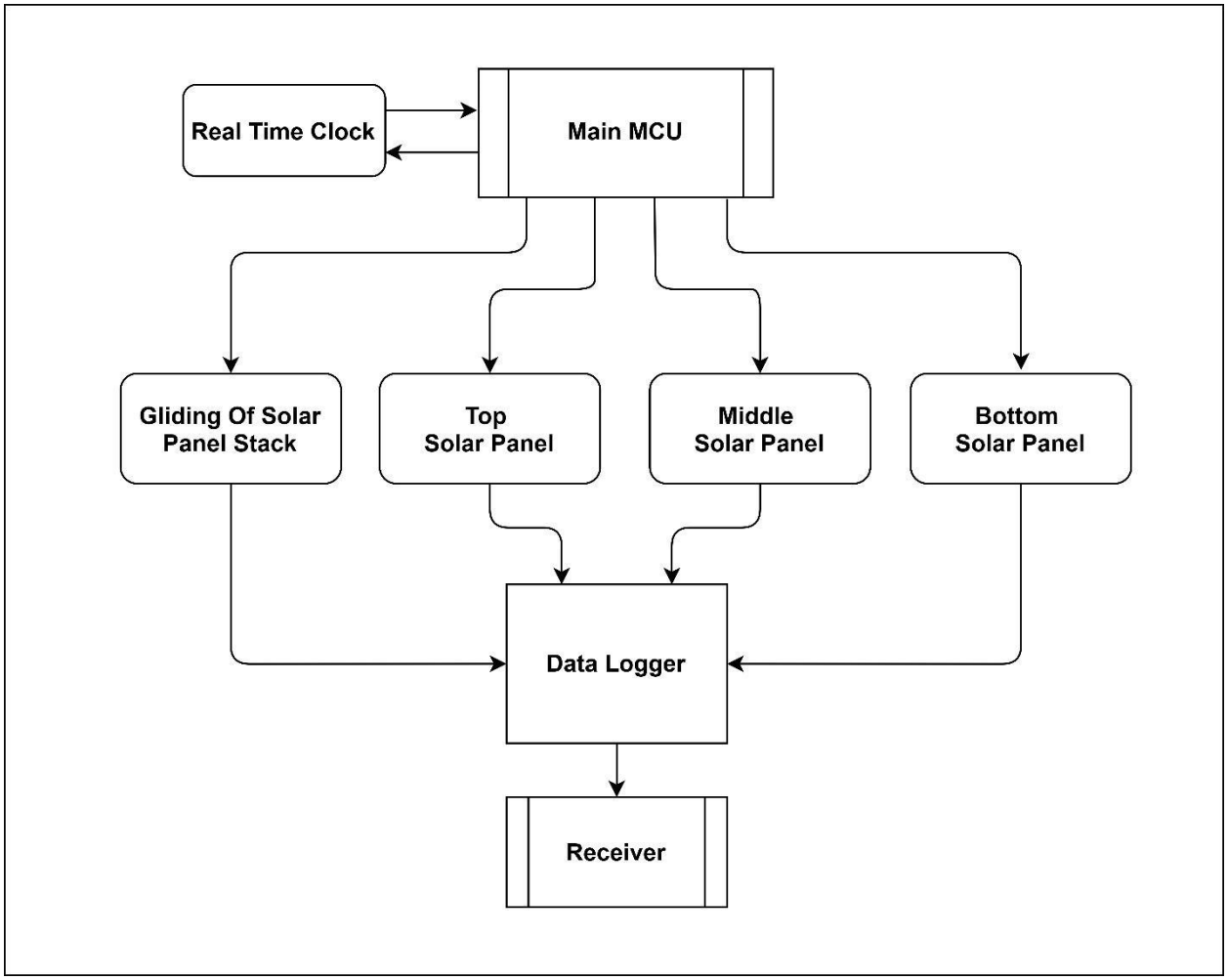


*Figure 25:Signal Flow Diagram*

The signal flow diagram of the multi-level solar panel system is sown in Figure25. The system consists of three solar panels namely top, bottom, and middle panel converts solar energy into electrical energy. The panels are rotated accordingly in phase with the sun's position by the microcontroller. The microcontroller reads the time from an RTC module and calculates the necessary steps to do so. The position of the gliding bar is controlled by an actuator. The actuator expands and compresses to control the lean angle of the gliding bar. The actuator is controlled by a set of the relay module. Finally, the output of the solar panels is measured using a data logger circuit and the data is stored into an SD card.

### 3.4.2.3. Control system circuit

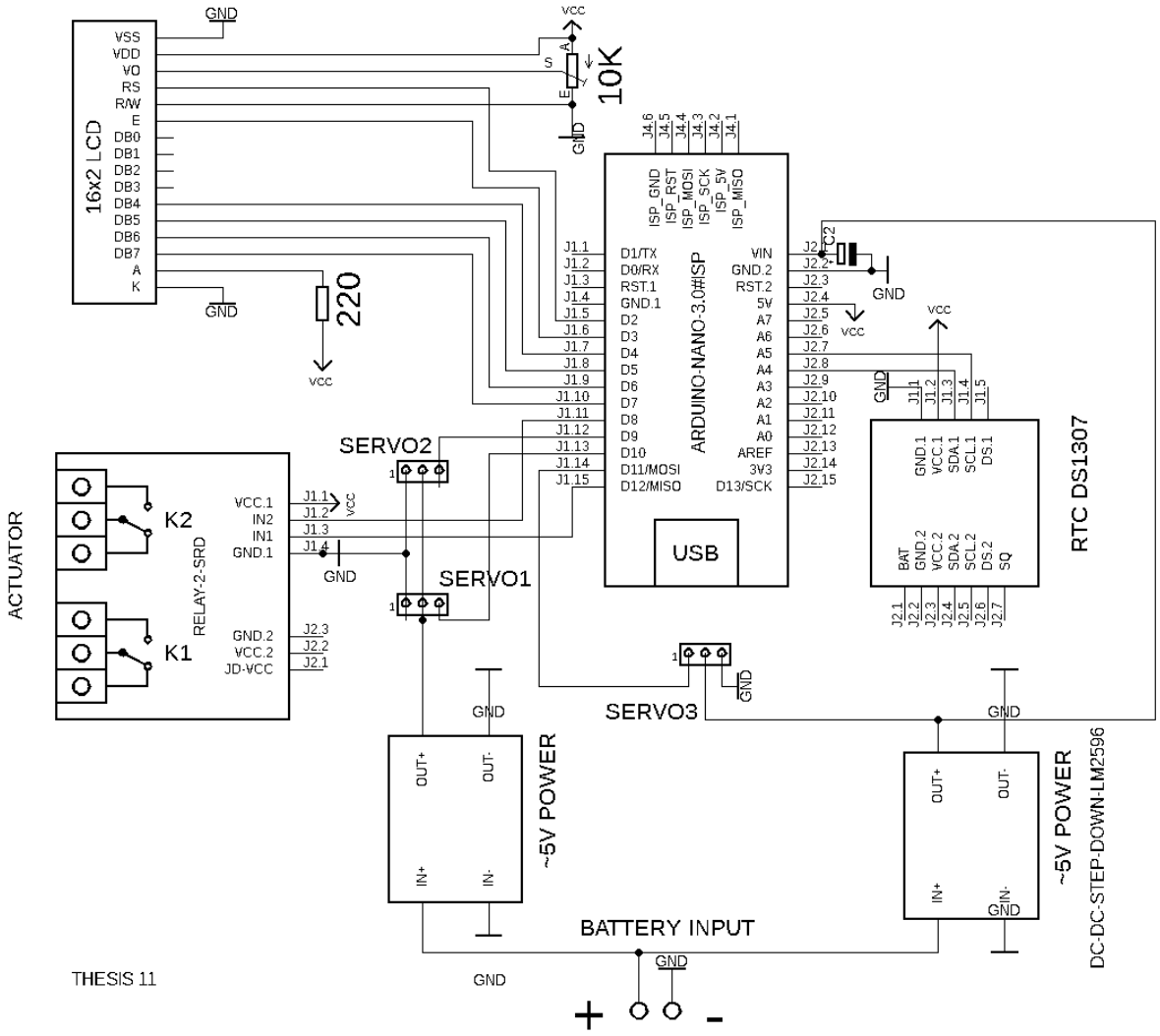


*Figure 26:Control Circuit Diagram*

Control circuit description:

In our project, we have used Arduino nano as the main microcontroller. Two Arduino nano is used in this system, one for the main solar panel control system and another for data logging purposes. In the solar panel control system, one dual-channel relay module, one RTC module, and three servo motors, and one Actuator is used. The relay module's input N1 and N2 are connected to the digital pins 5 and 7. The servo motors signal input pins are connected to the digital pin 7, 8, 9. The RTC (DS1307) module is connected using the analog pin A4 and A5.

For powering the components 12V is taken as the main input power source. Then two buck converters are used to step down the voltage to 5V. Buck converter 1 connected to the main power source supplies power for the servo motors and the relay module, which requires 5V as an input voltage. Additionally, buck converter 1 powers two servo motors and a relay module whereas, buck converter 2 is used to power one servo motor and the Arduino nano. RTC module connected to the microcontroller requires very low power, so it is directly connected to the Arduino 5V output pin. On the other hand, the actuator requires a very large portion of the power, so it is connected directly to the 12V power supply. We also kept an option of connecting an LCD module if required, which is also powered by the Arduino.

### 3.4.2.4. Data logger circuit

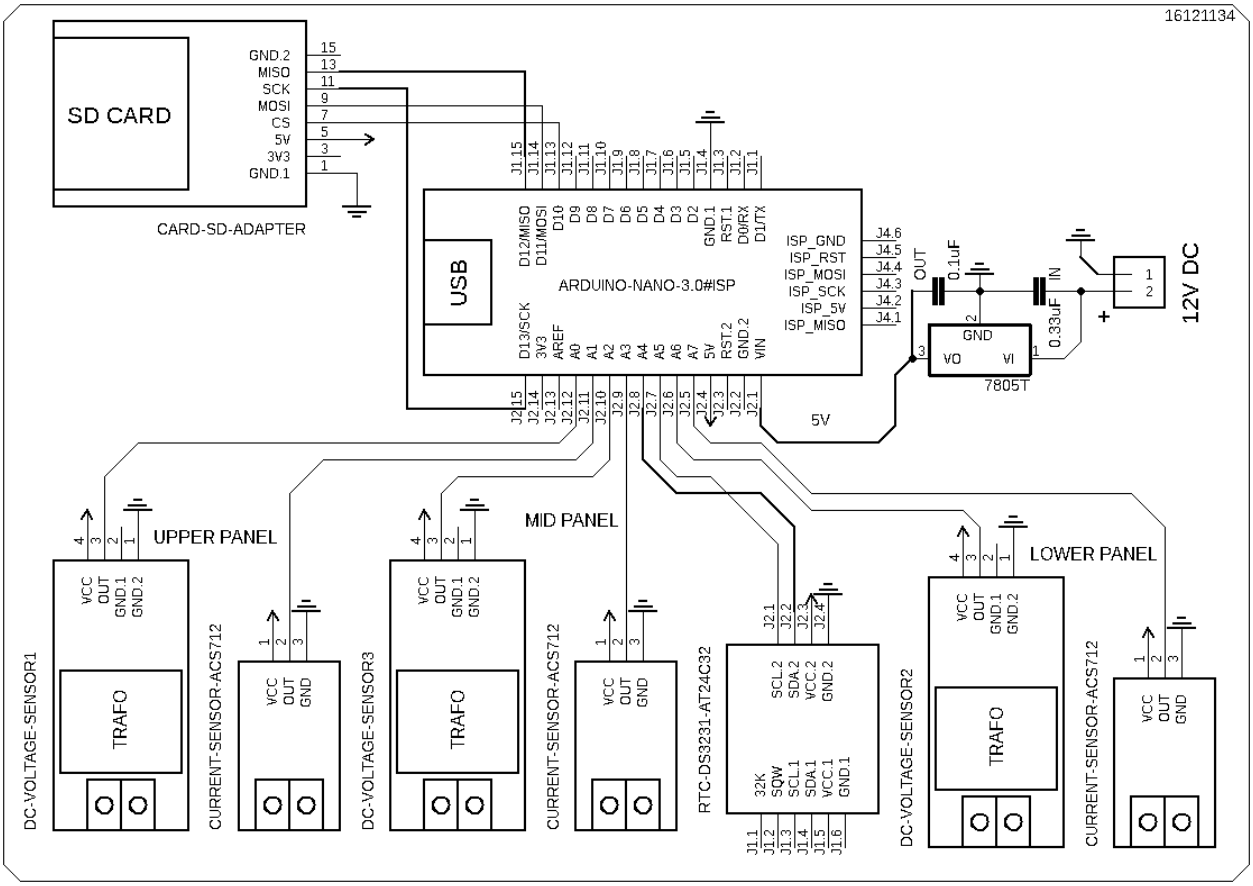


*Figure 27: Data logger Circuit Diagram*

Data logger circuit descriptions:

For data logging, we are using one Arduino Nano as the brain of the system. For data input, we are using three current and voltage sensors. Voltage and current sensors require analog input, so voltage sensors are connected to the analog pin A0, A2, A5. Current sensors are connected to the A1, A3, A7 pins. The data is indexed by time and date, so the RTC module is used for time and data input. The RTC module is connected to the SCL and SDA pin. After processing all the data, it is stored on an SD card. The SD card module is connected to the MISO, MOSI, and CLK pin. For powering the component 12V is taken as input. One voltage regulator is used

to convert 12V to 5V. 5V is sufficient to power all the components used here, so no additional supply is required.

# Chapter 4

## 4. Performance Analysis

A discrete comparison of mono-facial based multilevel solar panel system and bifacial based multilevel solar panel system is deliberated considering energy accumulation on a daily and monthly ground. Moreover, a separate comparison among mono-facial, bifacial mid panel and bifacial vertical panel for bifacial based multilevel solar panel system to have more obvious points for the proposed system. The yearly output system type is compared considering the effect of cloud and without cloud at the end of the discussion. Each of the system type alongside yearly electrical output is compared to get the percentage of difference.

## 4.1 Daily Energy Accumulation

Following results of our proposed model is based on the bifacial single axis tracking system:

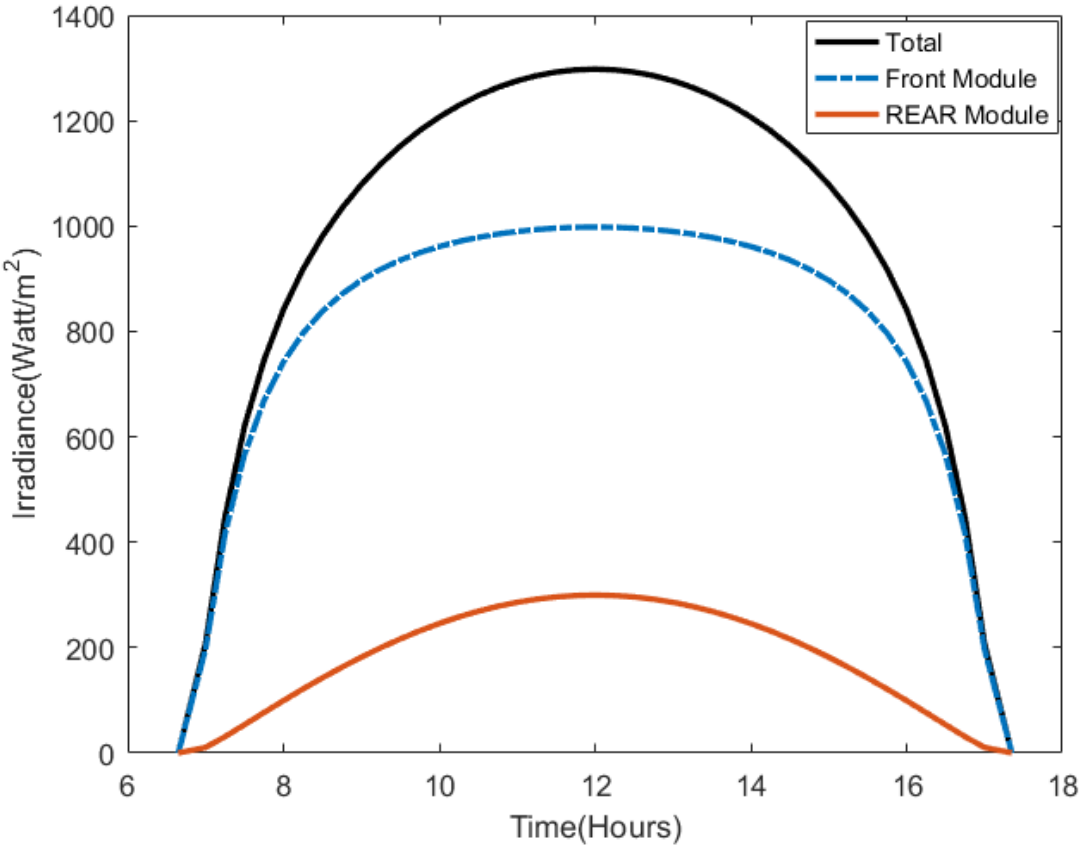


*Figure 28: Daily incident solar intensity of bifacial module based single axis tracker for a specific day Jan 15th*

Solar intensity on a regular basis is reckoned by the equations of chapter 2. However, for more clear explanation a single data considering January 15$^{th}$ is shown in all respects of the analysis in figure: 28

This means the solar intensity of bifacial based single axis tracking system is showing the results of January 15$^{th}$. In general, the mono-facial module output of the tracker is represented by the front panel of the bifacial module. Calculations show that the incident energy received by the front module is 8.5828 kWh/m$^2$ resulting in a sum total of 10.534 kWh/m$^2$ for the whole

bifacial single module. Moreover, we can observe from the figure that, rear side of the bifacial module contributes significant amount of energy into the system which upholds the importance of using bifacial module as the system produces 22.73% more energy than the mono-facial module.

Comparison between mono-facial and bifacial module:

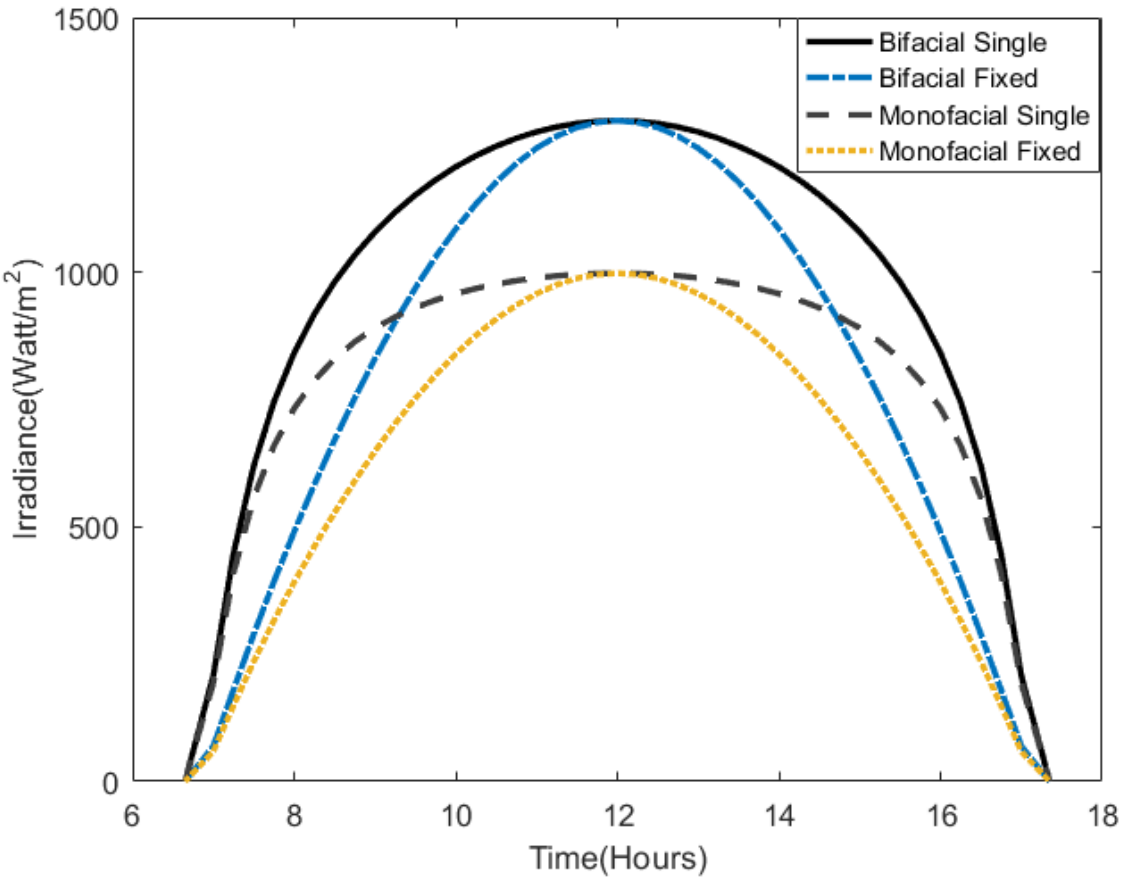


*Figure 29:Comparison of daily incident solar intensity of mono-facial and bifacial module*

In the figure 29, there is an analogy between mono-facial and bifacial solar intensity based on single and fixed axis tracking system respectively. Here, it is shown that the single axis tracker gathers more energy than the fixed axis tracker in both terms of Bifacial and Mono-facial module. In case of Mono-facial module the single module accumulate energy of 8.534 kWh/m$^2$ whereas the fixed module collects energy of 6.8024 kWh/m$^2$. Similarly, in case of bifacial module the single module gathers energy of 10.534 kWh/m$^2$ while the fixed module collecting energy of 8.7531 kWh/m$^2$. The outcome shows that Mono-facial single axis tracker harnesses 25.46% more energy comparing with the fixed axis tracker. Repeatedly, bifacial single axis tracker harnesses 20.35% more energy than the fixed one. To conclude, the single axis tracker is better than the fixed axis tracker in both cases of Mono-facial and Bifacial module. In addition, the bifacial single axis system is the better version of the whole system considering the accumulation of highest energy reckoning.

Energy comparison of Mono-facial, Bifacial mid panel and Bifacial vertical panel

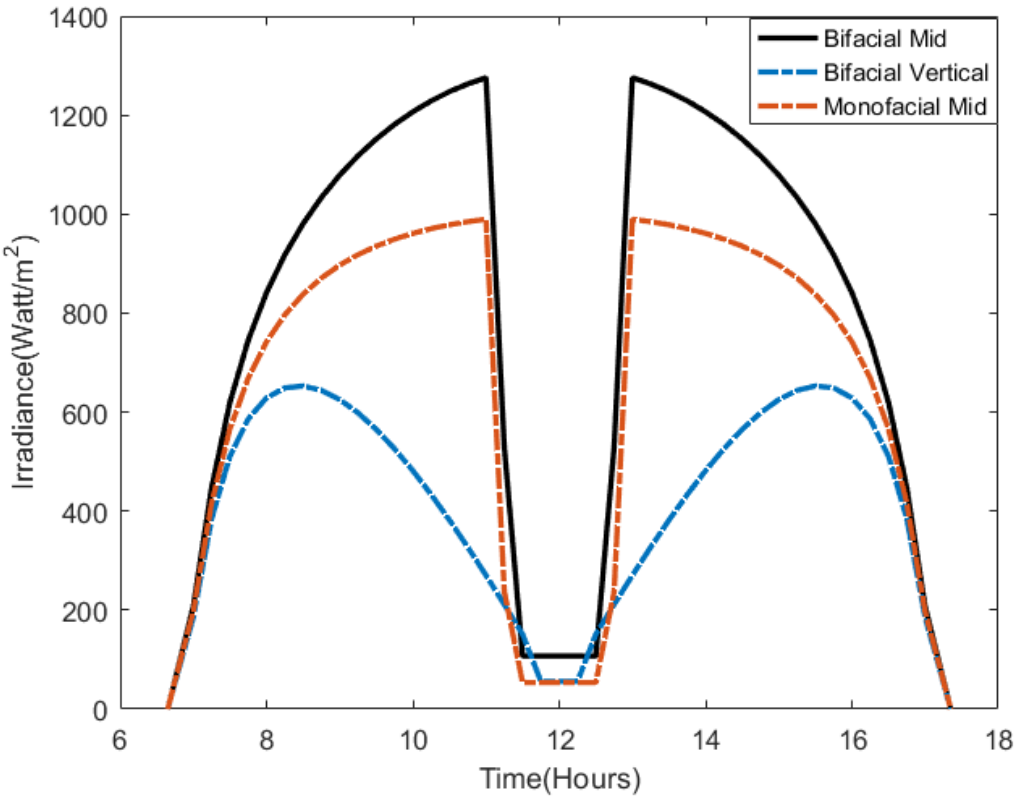


*Figure 30:Comparison of daily incident solar intensity of Mono-facial and Bifacial mid panel and Bifacial vertical panel*

Bifacial module has advantages as it gathers energy from the two sides of the module. Therefore, this module can set up regular fixed horizontal or vertical framework. The most usually utilized framework is vertically mounted module seen on the roadsides. The incident energy of Bifacial vertical is lower than Bifacial mid module. However, the direct irradiance to the panel is highest during the earlier part of the morning time. Hence, a stiffness is observed during sunrise and sunset time. After the earlier part of the morning the direct irradiance becomes lower till noon so the vertical panel cannot harness the solar power as expected. During this time only diffused irradiation is harnessed on both sides of the bifacial module. The energy from this vertical system is 4.448kWh/$m^2$.

The Multilevel Bifacial solar panel system having top module, mid module and bottom module where the mid module gets shaded from the top module at noon. Therefore, till 11 am the system works like a single axis tracker in the bifacial system. After 11 am to 1 pm the position of the middle panel will be in a vertical manner although it will get only diffused irradiation on the both sides of the panel as it is shaded by the top panel. This process will add an impact on the total output as the energy from this bifacial middle panel considering its position is 8.67kWh/$m^2$.

During 11am to 1pm the mid panel of the multilevel Mono-facial solar panel system follows the same procedure to harness energy as the bifacial solar panel system. The diffused irradiance will work only on the single side in this case. For the rest of the time the system works like a single axis tracker in the Mono-facial system. 7.025kWh/$m^2$ energy is collected in this procedure. The comparison shows that the bifacial middle panel can raise 23.42% more energy than the Mono-facial middle panel.

Energy calculation of the Multilevel Mono-facial system

Daily incident energy:

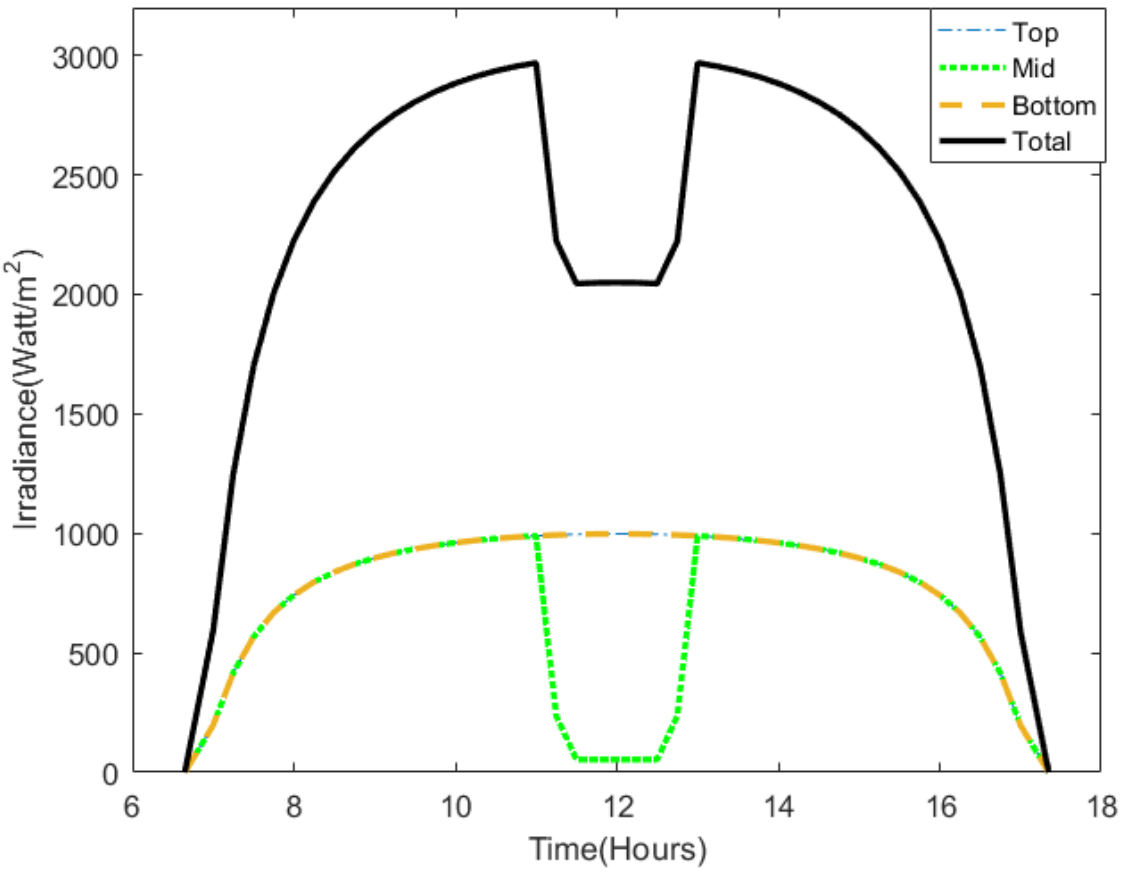


*Figure 31:Mono-facial multilevel output comparison for January 15*

There are 4 plots shown in the figure 31. Considering the 3 panels of the Mono-facial multilevel system along with the total Irradiance of the full system. The top and the bottom panel gather the exact same power resulting the overlapping showing in the figure. However, the middle panel cannot collect the same energy as the system's position is in a vertical manner during the time of 11am to 1am.There is no boosting effect considering the mono-facial structure. The solar energy harnessed by the three panels are shown in the Table.10

| Solar Panel | Energy (kWh/m$^2$) |
|---|---|
| Mono-facial energy top | 8.5828 |
| Mono-facial energy mid | 7.0253 |
| Mono-facial energy bottom | 8.5828 |
| Total | 24.191 |

*Table 10: Multilevel Mono-facial system energy for January 15*

Energy calculation of the proposed system:

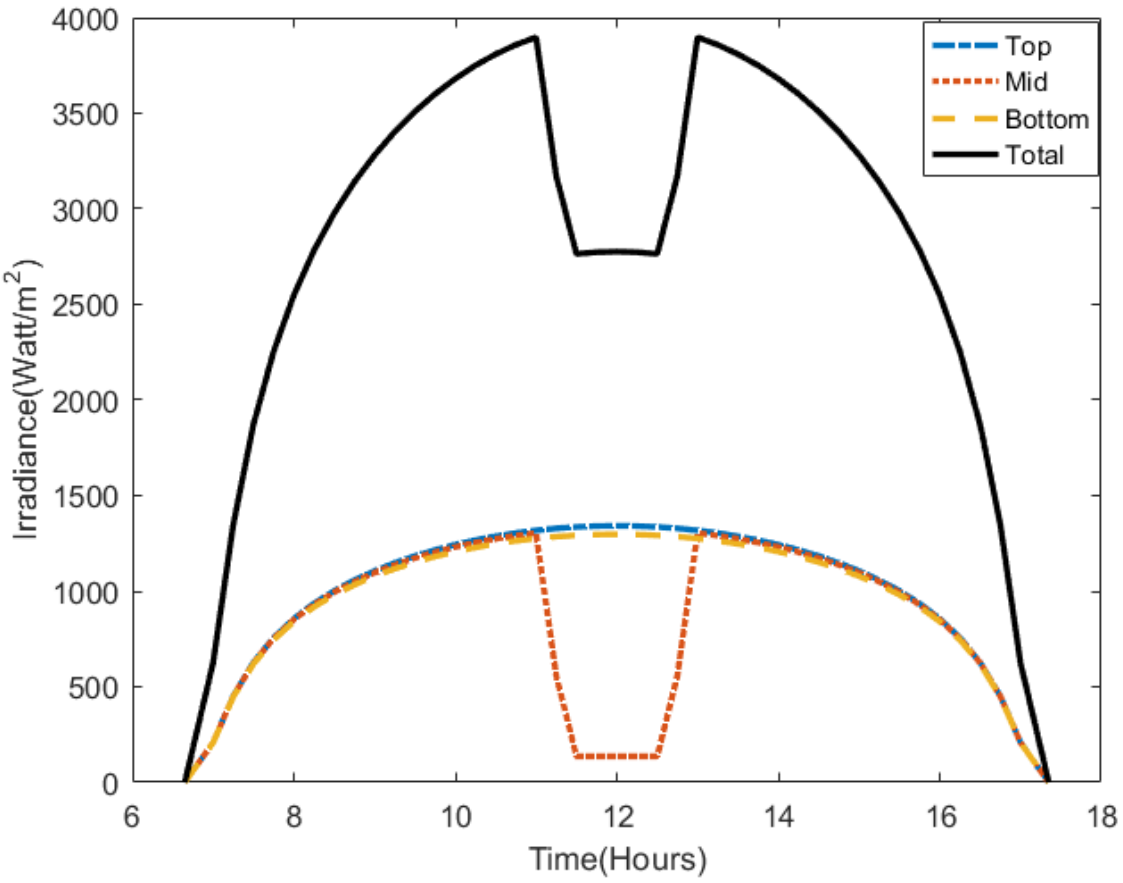


*Figure 32:Bifacial multilevel output for January 15*

There are 4 plots shown in the figure 32. Considering the 3 panels of the Bifacial multilevel system along with the total irradiance of the full system we observe that the top and the bottom panel absorb almost the same amount of power where the reflected solar irradiance boost up to 15% on the rear side only for the upper panel. 10% boost up is the outcome for the middle panel as the middle panel stays on a vertical position during 11am to 1pm. In the figure the top-level panel shape is slightly higher than the bottom level panel and the shape of the middle panel takes a dip. However, significant amount of energy is harnessed from all the three panels individually shown in the Table11

| Solar Panel | Energy ($kWh/m^2$) |
|---|---|
| Bifacial energy top | 10.823 |
| Bi -facial energy mid | 8.8630 |
| Bi -facial energy bottom | 10.534 |
| Total | 30.220 |

*Table 11: Proposed system energy for January 15*

Cumulative energy calculation of the proposed systems:

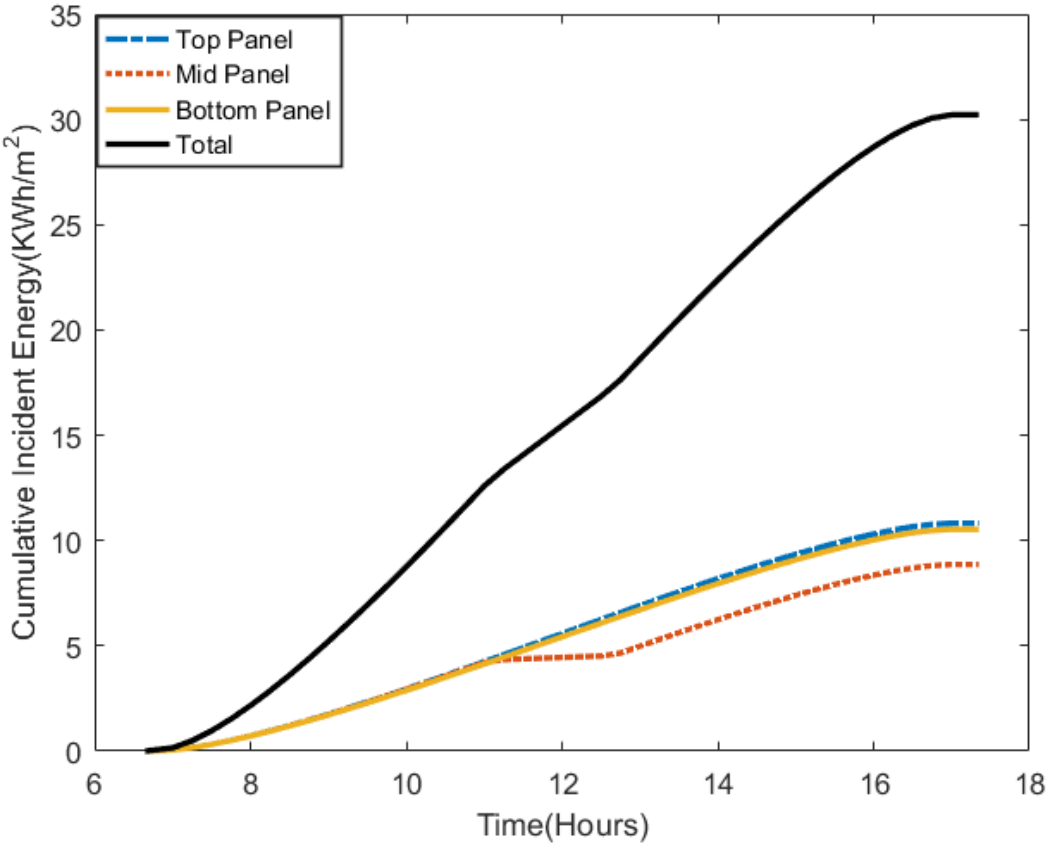


*Figure 33: Bifacial multilevel output for January 15*

The cumulative energy of the 3 panels is shown the figure (33) as the time increases. The upper panel and the bottom panel give a graphical increase in the energy slope output as the day goes by. On the other hand, the middle panel energy slope decreases as the panel gets vertical for a certain amount of time declaring the time period of 11 am to 1 pm. The total energy as the time increases during the day is reckoned 30.22 KWh/m$^2$.

## 4.2 Monthly Energy Accumulation

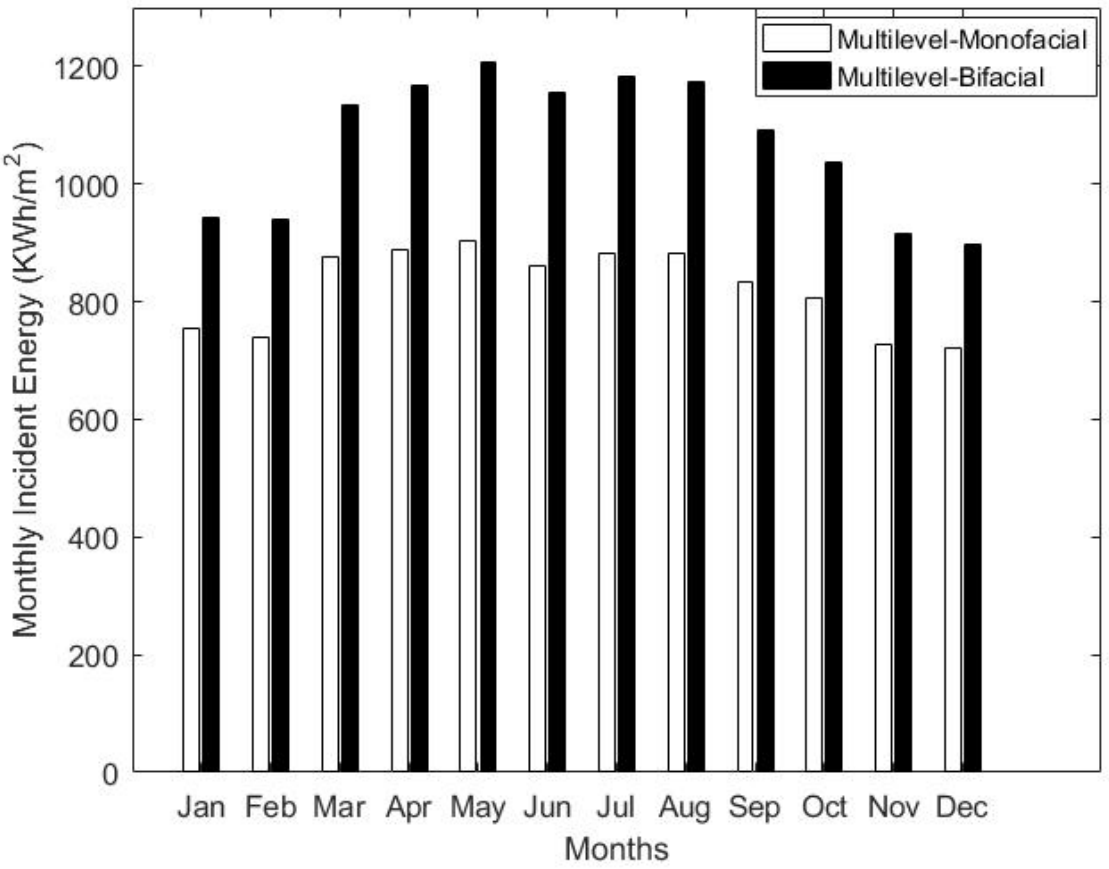


*Figure 34:Comparison of monthly incident solar intensity of mono and bifacial module based multilevel solar panel system without cloud impact energy of the different panels of Bifacial multilevel system output on January 15*

Here in figure 34, a comparison of monthly incident energy is shown between mono-facial and bifacial module of the proposed system. Environmental impact specifically cloud impact is not considered here. From the analysis it shows that energy accumulation is higher during summer season due to the position of the sun. Whereas, during the time of winter energy harnessing is considerably low. From the calculations, the yearly energy harnessing for bifacial module is 12.8456 MWh/$m^2$. For Mono-facial, the amount of energy collection is 9.8770 Mwh/$m^2$. The bifacial module gets 30.06% more energy than the mono-facial module considering the values that we have got from the calculations.

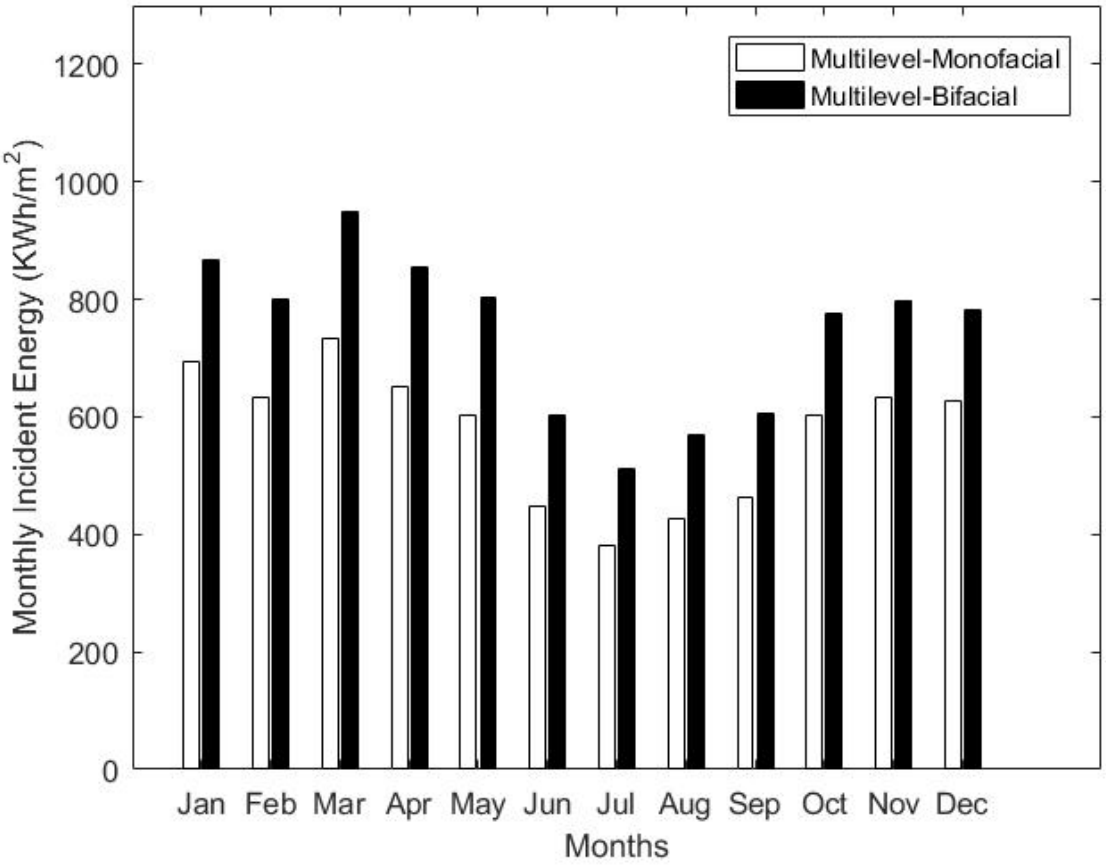


*Figure 35:Comparison of monthly incident solar intensity of mono and bifacial module based multilevel solar panel system with cloud impact*

A comparison of monthly incident energy is shown between mono-facial and bifacial module of the proposed system considering the cloud impact is shown in figure 35. As the cloud impact is considered here the results depict that the moderately high energy is collected during the time of March to May. During the time of June to September the energy is harnessed comparatively low. Here in this process, the yearly energy calculations for bifacial module is 8.9209 MWh/$m^2$ and the Mono-facial module is 6.8956 MWh/$m^2$. Considering the cloud impact the multilevel bifacial gets 29.37% more energy than the Mono-facial system making the bifacial module considered to be forward.

**Electrical Output considering Cloud cover**

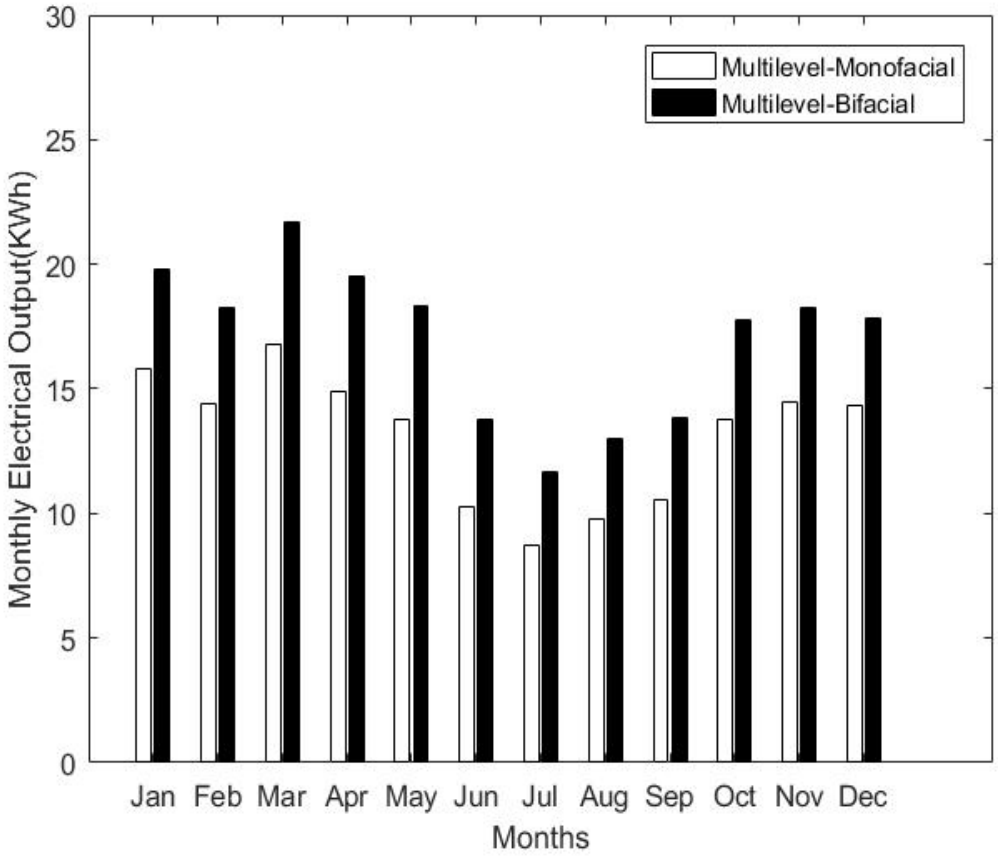


*Figure 36: Comparison of monthly electrical output of mono and bifacial module based multilevel solar panel system considering cloud impact*

Electrical output on monthly order is shown in figure (36) considering the cloud as an environmental impact. Using the formula of electrical output[28], we get the result for Mono-facial system is 0.1575 MWh/$m^2$. On the other hand, the bifacial module collects 0.2038 MWh/$m^2$ of energy. Here, the bifacial module gets 29.40% more energy than the mono-facial multilevel module.

| System Type | Yearly Output without cloud effect ($MWh/m^2$) | Yearly Output with cloud effect ($MWh/m^2$) | Yearly Electrical output with cloud effect ($MWh/m^2$) |
|---|---|---|---|
| Mono-facial Multilevel Solar Panel System | 9.8770 | 6.8956 | 0.1575 |
| Bifacial Multilevel Solar Panel System | 12.8456 | 8.9209 | 0.2038 |
| Percentage of difference | 30.06% | 29.37% | 29.40% |

*Table 12:Overall comparison of different type of system based on yearly output*

Electrical Output considering Cloud cover

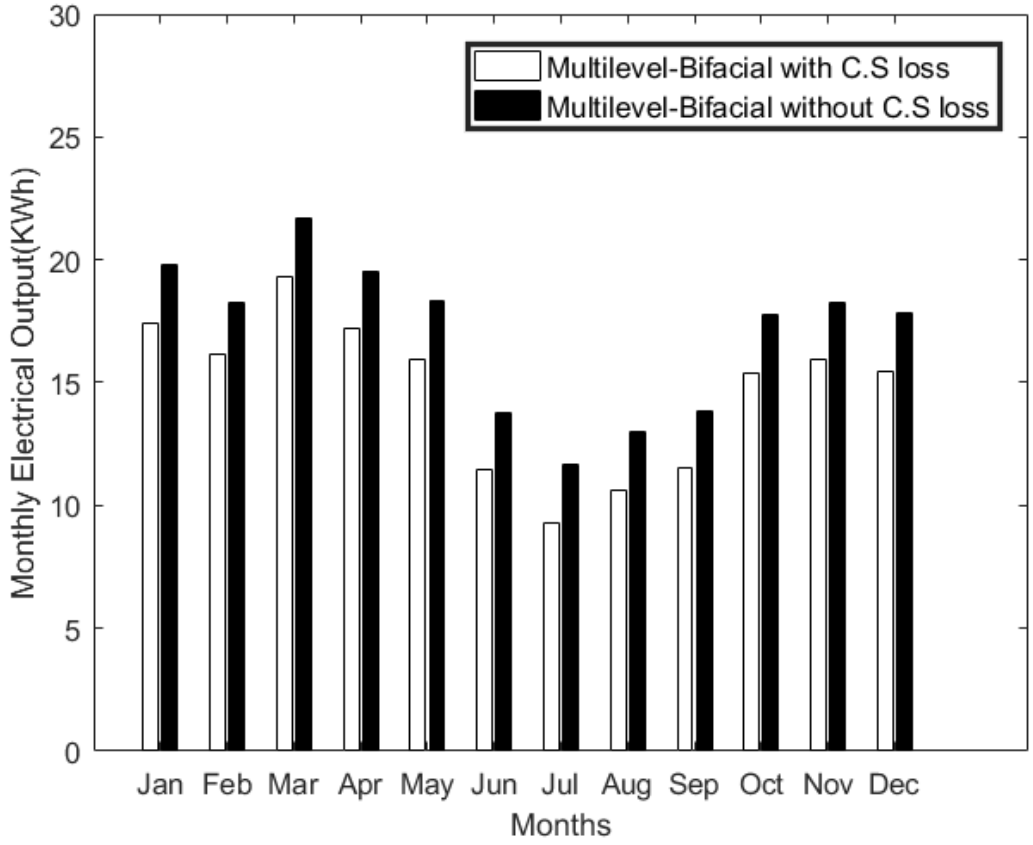


*Figure 37:Comparison of Control System Loss (monthly) electrical output of multilevel bifacial module based multilevel solar panel system*

The yearly electrical energy output with environmental impact of the proposed system is 0.2038 MWh. After deducting the control system (C.S) energy consumption, the final energy output is 0.1757 MWh. The monthly comparison between generated energy with and without control system loss considering environmental impact has been illustrated in figure 37.

## Conclusion

When the typical solar panel system has already reached its maximum capacity to generate energy, a newly designed system to increase the energy efficiency rate and studied to show its performance in the stated research work. From Chapter 4, we get the daily and monthly energy accumulation with a cumulative analysis of yearly energy accumulation of bifacial multilevel solar panel systems. The result analysis shows that a bifacial multilevel solar panel produces 29.37% more energy than a single mono-facial multilevel solar panel. We have also compared the results with the theoretical estimation and previous data available on multilevel solar panel systems. After successfully boosting the electrical output by a significant margin, this research will play a significant role to construct a better multilevel solar system for urban areas.

## Future Scope of this research

The implement of height boosting and albedo factor carries a vital role in this research, which has a few researches available in our country. It requires certain researches to establish the totally reflected radiance on any collector panel. Calculation of the irradiance on the collector panel comprises several factors, and the generalized albedo factor selection might give a fractional difference in terms of cumulative energy and study regarding this specific topic is necessary. For further research on this subject is relatively important, as converting this generous amount of solar energy into electrical energy would do much good. As the conventional energy sources are finite & fast depleting, an improved multilevel solar power system will simultaneously convert sunlight into electricity by photovoltaic.

## Reference


[1] *The World Bank Group*. (2017, 11 13). Retrieved from Data World bank:

https://data.worldbank.org/indicator/EG.ELC.ACCS.ZS?locations=BD

[2] S. A. M. K. R. M. R. Ahmed Hosne zenan, "A new multilevel Solar panel System for Urban Areas," in Developments in Renewable Energy Technology (ICDRET) 2014 3rd International Conference, 2013.

[3] Hoque, Sumaiya & Das, Bably & Al Askary, Md. Abu Hasan. (2019). Comparative Analysis of Dual and Single Axis Solar Tracker.

[4] Coba F, Aguilera J, Korbee N, de Gálvez MV, Herrera-Ceballos E, Álvarez-Gómez F, Figueroa FL. UVA and UVB Photoprotective Capabilities of Topical Formulations Containing Mycosporine-like Amino Acids (MAAs) through Different Biological Effective Protection Factors (BEPFs). Mar Drugs. 2019 Jan 14;17(1):55. doi: 10.3390/md17010055. PMID: 30646557; PMCID: PMC6356945de la.

[5]"(PDF) Solar Highway in Bangladesh Using Bifacial PV." https://www.researchgate.net/publication/329134858_Solar_Highway_in_Bangladesh_Using_Bifacial_PV

[6] "Virtual Sensing of Photovoltaic Module Operating ...." https://www.researchgate.net/publication/339581169_Virtual_Sensing_of_Photovoltaic_Module_Operating_Parameters

[7] "Single-Diode and Two-Diode Pv Cell Modeling Using Matlab ...." https://www.researchgate.net/publication/281942470_Single-Diode_and_Two-Diode_Pv_Cell_Modeling_Using_Matlab_For_Studying_Characteristics_Of_Solar_Cell_Under_Varying_Conditions.

[8] Duffie, J. A., & Beckman, W. A. (2013). Solar engineering of thermal processes (4th ed.). Hoboken, N.J.: John Wiley & Sons

[9] G.M. Masters, “Renewable and efficient electric power systems”, 2004,

New jersey: John Wiley & Sons, Inc.

[10]Jakhrani, Abdul & Othman, Al-Khalid & Rigit, Andrew & Samo, Saleem & Kamboh, Shakeel. (2012). Estimation of Incident Solar Radiation on Tilted Surface by Different Empirical Methods. International Journal of Scientific and Research Publications. 2. 1-6.

[11]Durusoy, B., Ozden, T. & Akinoglu, B.G. Solar irradiation on the rear surface of bifacial solar modules: a modeling approach. Sci Rep 10, 13300 (2020). https://doi.org/10.1038/s41598-020-70235-3

[12]Liu, B Y.H., & Jordan, R C. Interrelationship and characteristic distribution of direct, diffuse, and total solar radiation. United States. https://doi.org/10.1016/0038-092X(60)90062-1

[13]Daut, M. Irwanto, Y. M. Irwan, N. Gomesh and N. S. Ahmad, "Clear sky global solar irradiance on tilt angles of photovoltaic module in Perlis, Northern Malaysia," International Conference on Electrical, Control and Computer Engineering 2011 (InECCE), Pahang, 2011, pp. 445-450, doi: 10.1109/INECCE.2011.5953923

[14]Marion, W. F., & Dobos, A. P. Rotation angle for the optimum tracking of one-axis trackers.

[15]Appelbaum, J., 2018. "The role of view factors in solar photovoltaic fields," Renewable and Sustainable Energy Reviews, Elsevier, vol. 81(P1), pages 161-171.

[16] M. R. Shaikh, "A Review Paper on Electricity Generation from Solar Energy," International Journal for Research in Applied Science and Engineering Technology, vol. 887.

[17]S. N. I. a. M. R. T. Debnath, "Implementation of an RTC based multilevel solar panel system," in 2017 IEEE Region 10 Humanitarian Technology Conference (R10-HTC), Dhaka, 2017

[18]Mohammadi, K. ., Sabory, N. R. ., Karimi, K. ., Ahmadi, M. ., Danish, M. S. S. and Senjyu, T. (2020) “Performance evaluation of different photovoltaic (PV) modules: A case study ”, Journal of Engineering and Technology Revolution. Okinawa, Japan, 1(1), pp. 1-8. doi: 10.37357/1068/jetr/1.1.01.

[19]Tamrakar, Vivek & Gupta, S.C. & Sawle, Yashwant. (2015). Study of characteristics of single and double diode electrical equivalent circuit models of solar PV module. 312-317. 10.1109/ICESA.2015.7503362

[20]MODULES, S. (2016). CALCULATING THE ADDITIONAL ENERGY YIELD OF BIFACIAL SOLAR MODULES.

[21]Quer, J. C. (2014). *Arduino Uno - Octopart*. Retrieved from Datasheet.octopart: https://datasheet.octopart.com/A000066-Arduino-datasheet-38879526.pdf

[22]"Real-Time Clocks - Basic Electronics Tutorials." https://www.electronics-tutorials.ws/connectivity/real-time-clocks.html.

[23]"LINEAR ACTUATOR LIGHT DUTY SERIES - Pololu Robotics and ...." https://www.pololu.com/file/0J1238/LD-Linear-Actuator-Data-Sheet.pdf."(PDF)

[24]"How Do You Size a Linear Actuator? - firgelliauto.com." https://www.firgelliauto.com/blogs/news/how-do-you-size-a-linear-actuator.

[25]"Relay Channel - an overview | ScienceDirect Topics." https://www.sciencedirect.com/topics/engineering/relay-channel.

[26]"Relay Module 2-Channel MR009-004 - MakerZONE." https://www.makerzone.store/wp-content/uploads/2016/01/mr009-004_datasheet.pdf.

[27] Brock LeBaron, Inge Dirmhirn, "Strengths and limitations of the Liu and Jordan model to determine diffuse from global irradiance",Solar Energy,Volume 31, Issue 2,1983,Pages 167-172,ISSN 0038-092X,

[28] https://www.lg.com/es/download/resources/CT32016002/CT32016002_1763.pdf

## Appendix A.

```
A=asind((sind(a)*sind(l))+(cosd(a)*cosd(l)*cosd(ws)));

AM= (1/cosd (Za));

bft=acosd(cosd(ws)*cosd(23.5))

fi2=asind(sind(ws)/(sind(bft))) ;

fys=asind((cosd(a)*sind(ws))/cosd(A));

kosh= (cosd(A)* cosd(fys-fi2)*sind(bft))+(sind(A)*cosd(bft));
beta=bft;
refactprear = ((1+cosd(beta))/2);
difactmrear = ((1-cosd(beta))/2);
difactmf = ((1+cosd(beta))/2);
Ib = AA*(exp(-kk*AM));
Idrect(i) = Ib*kosh;
idtrear = cc*Ib*difactmrear;
irtrear = alb*Ib*(sind(A)+cc)*refactprear;
idtfront = cc*Ib*difactmf;

Za=90-A;
```

## Appendix B.

```
void sunrise() {
double del = 23.45 * sin(360 * pi / 180 / 365 * (N + 284));
double Ws = acos(-tan(lattitude * pi / 180) * tan(del * pi / 180)) * 180 / pi;
double AST = 720 - Ws * 4;
double LSTM = 15 * round(longitude / 15);
double D = 360 * pi / 180 * (N - 80) / 365;
double ET = 9.87 * sin(2 * D) - 7.53 * cos(D) - 1.5 * sin(D);
SRT = AST - 4 * (LSTM - 90.25) - ET;
}

//sunset time calculation
void sunset() {
double del = 23.45 * sin(360 * pi / 180 / 365 * (N + 284));
double Ws = -acos(-tan(lattitude * pi / 180) * tan(del * pi / 180)) *180/pi;
double AST = 720 - Ws * 4;
double LSTM = 15 * round(longitude / 15);
double D = 360 * pi / 180 * (N - 80) / 365;
double ET = 9.87 * sin(2 * D) - 7.53 * cos(D) - 1.5 * sin(D);
SST = AST - 4 * (LSTM - 90.25) - ET;
}
```